

## MASTER

### Identification of heart surface potentials from skin potentials with conditions

van Kemenade, F.

*Award date:*  
1978

[Link to publication](#)

#### **Disclaimer**

This document contains a student thesis (bachelor's or master's), as authored by a student at Eindhoven University of Technology. Student theses are made available in the TU/e repository upon obtaining the required degree. The grade received is not published on the document as presented in the repository. The required complexity or quality of research of student theses may vary by program, and the required minimum study period may vary in duration.

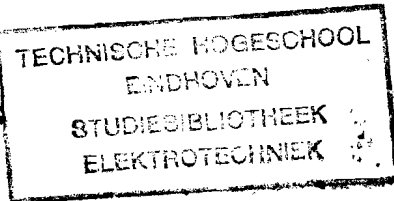
#### **General rights**

Copyright and moral rights for the publications made accessible in the public portal are retained by the authors and/or other copyright owners and it is a condition of accessing publications that users recognise and abide by the legal requirements associated with these rights.

- Users may download and print one copy of any publication from the public portal for the purpose of private study or research.
- You may not further distribute the material or use it for any profit-making activity or commercial gain

3014 b5e

EINDHOVEN UNIVERSITY OF TECHNOLOGY  
THE NETHERLANDS  
DEPARTMENT OF ELECTRICAL ENGINEERING  
GROUP MEASUREMENT AND CONTROL



IDENTIFICATION OF HEART SURFACE  
POTENTIALS FROM SKIN POTENTIALS  
WITH CONDITIONS

by: F. van Kemenade

Submitted in partial fulfillment of the requirements for the degree of Ir. (M.Sc.) at the Eindhoven University of Technology. The work was carried out from December 1977 until October 1978 under the directorship of Prof. dr. ir. P. Eykhoff. Advisor was Ir. A.A.H. Damen.

---

SUMMARY

The relation between the epicardial potentials and skin potentials can be given, under certain assumptions, by a linear transformation by means of a transfer matrix. When a mathematical operation, called the Singular Value Decomposition, is performed on this transfer matrix, components are found that can be interpreted as fundamental potential distributions over the heart surface and over the skin. Each fundamental potential distribution over the epicard is related to a corresponding fundamental potential distribution over the skin via a transfer coefficient. Such a transfer coefficient is a measure for the observability of the corresponding fundamental epicardial potential distribution in the skin potentials. The distributions on the epicard with the worst observability cause skin potentials, which lie below the noise level, so that they can not be obtained from skin measurements.

In order to reduce the influence of the noise, the worst observable distributions should be ignored in the inverse calculation of the epicardial potentials from the measured skin potentials. By rejecting these distributions a number of degrees of freedom is obtained. These degrees of freedom shall be used to estimate the epicardial potentials better with the help of the a priori information about the electrical heart activity.

The results, derived from simulated skin potentials, were well-promising. However, the results, derived from measured skin potentials, did not meet expectations. The main reason of this bad estimation is a not correct transfer matrix. Therefore it is necessary to determine exactly the geometry and position of the heart in the body and to take the inhomogeneities into account, in order to obtain in practice better results.

CONTENTS

	page
<u>SUMMARY</u>	2
<u>1. INTRODUCTION</u>	5
<u>2. PHYSICAL MODELLING OF THE HUMAN BODY AND THE DISPLAY OF THE DATA</u>	7
2.1. The physical model of the human body	7
2.2. Definition of a point distribution on the torso and on the heart.	7
2.3. Presentation of the potentials on a closed surface.	10
<u>3. MATHEMATICAL DESCRIPTION OF THE PROBLEM</u>	12
3.1. Introduction of the Singular Value Decomposition (S.V.D.).	12
3.2. The S.V.D. applied to the heart-to-skin transfermatrix.	12
3.3. The influence of the noise in the skin potentials.	14
3.4. Estimation of the epicardial potentials with the help of the a priori information.	17
<u>4. ESTIMATION OF THE EQUIVALENT DOUBLE LAYER FROM SIMULATED SKIN POTENTIALS</u>	21
4.1. The simulated double layer on the heart surface.	21
4.2. The transfermatrix relating double layer intensities to skin potentials.	23
4.3. Estimation of the equivalent double layer.	24
4.3.a Results in noisefree case.	24
4.3.b Results in noisy case.	27
<u>5. ESTIMATION OF THE EPICARDIAL POTENTIALS FROM MEASURED SKIN POTENTIALS</u>	35
5.1. The Electrocardiogram ( ECG ).	35
5.2. The transfermatrix relating epicardial potentials to skin potentials.	36
5.3. Results.	38
<u>CONCLUSIONS</u>	41
<u>LITERATURE</u>	43
<u>ACKNOWLEDGEMENTS</u>	45
<u>APPENDIX:</u> Notes about the calculation of the transfermatrix relating equivalent double layers to skin potentials.	46

	page
<u>ANNEX 1.</u> The course of the equivalent double layer on the heart surface.	48
<u>ANNEX 2.</u> The course of the equivalent double layer in the points on the left ventricle.	49
<u>ANNEX 3.</u> The course of the equivalent double layer in the points on the right ventricle.	50
<u>ANNEX 4.</u> Part of the estimated source distributions on the heart in the simulated noise-free case.	51
<u>ANNEX 5.</u> Part of the simulated source distributions on the heart.	52
<u>ANNEX 6.</u> Part of the estimated source distributions on the heart in the simulated noisy case.	53

## 1. INTRODUCTION

This study forms part of a project in the group " Measurement and Control", Department of Electrical Engineering at the University of Technology in Eindhoven. The goal of this project is trying to identify the electric phenomena, that precede the heart contraction of a human on the basis of non-invasive measurements. The significance of these investigations is, that, if the sources of the electrical heart activity would be known, this would present a good indication for the condition of the heart and a help to diagnose diseases of the heart, possibly in an early stage, where these electrical sources are disturbed. The identification will be performed on a set ECG's (= electrocardiograms) and torso geometry data. In this report only the contraction of the ventricles will be discussed, because this phenomenon is well measurable on the skin.

It is obvious, that an exact calculation of a three dimensional source distribution over the heart from the two dimensional skin potential distribution is not possible. This can be illustrated by the fact, that an observer outside the source area can not distinguish the field of a point charge from the field of a homogeneous charged sphere in a unbounded homogeneous medium. This problem can be avoided, if, instead of the three dimensional source distribution over the heart, a two dimensional epicardial potential distribution is calculated from the two dimensional skin potential distribution. These epicardial potentials are caused by the electrical heart activity on the outer surface of the heart.

In order to limit the calculations of the epicardial potentials from the skin potentials, it is necessary to make some assumptions about the human body and heart. In this study the body will be supposed to be a linear, homogeneous and isotropic medium, as far as the electric fields are concerned. This means, that the inhomogeneities, such as lungs, liver, bones, etc. have not been accounted for in this model. The influence of the body-extremities (head, arms, legs) is neglected, which is allowed, because hardly any current will enter these extremities as the torso resistancy is sufficiently low. As no reliable measurements of the geometry of the heart were available, the heart will be approximated by a sphere, which encloses the heart tightly.

The skin potentials are measured in about a hundred points on the torso ( see chapter 2, figure 2 ), while the epicardial potentials are calculated in 66 points on the epicard. The number of points on the heart surface should be less or equal to the number of points on the skin, because the potentials on the heart surface can not be more detailed than the skin potentials from which they are derived. To make this calculation possible on a digital computer, the skin potentials were measured by taking samples with an interval time of 3 msec.

The noise on the measured skin potentials shall play an important part in this study. Namely, it is not possible to calculate the epicardial potentials reliably, when the skin potentials contain some noise. However, it is possible to reduce the influence of the noise in the inverse calculation of the epicardial potentials from the skin potentials with the help of a priori knowledge of the depolarisation-wave.

The possibility of introducing this a priori information in the inverse calculation depends upon a rigid definition of the degrees of freedom, which are left out, when the information of the skin potentials have been used. A mathematical technic, called the Singular Value Decomposition ( S.V.D. ), applied on the transfer matrix offers us a possibility of a distinction between the degrees of freedom depending on skin potentials on one hand and the degrees of freedom to be determined by a priori information on the other hand. This S.V.D. will briefly be discussed in chapter 3. If the S.V.D. has been applied on the transfer matrix, that relates epicardial potentials to skin potentials, then the decomposition results in components, that can be interpreted as independent fundamental potential distributions over the epicardial surface and over the skin. The singular values, which result from the S.V.D., will appear to be a measure for the contribution of a fundamental distribution over the heart surface to the total skin potentials. The observability of such a fundamental epicardial potential distribution is so much the better, if the corresponding singular value is greater. Consequently only those distributions on the heart surface can be estimated reliably from the skin potentials, if the signal to noise ratio of the distributions is greater than 1. So, if the distributions on the heart surface, that cause skin potentials below the noise level will be rejected, the influence of the noise will be less.

It is obvious, that in this way the epicardial potentials can not be calculated well. In order to estimate these potentials better, the a priori information about the electrical heart activity will be used. This a priori information exists among other things of the following approximations:

- the atria shall be regarded as inactive during the QRS-complex with respect to the ventricles, whose activity is far dominant;
- each area of the heart muscle depolarises only once per heart cycle;
- each area of the ventricles has to depolarize;
- the polarity of the potential difference over the heart wall is fixed during the depolarisation and the amplitude is constant.

In what way this a priori information can be used to estimate the epicardial potentials better is described in chapter 3.

In order to check the theory, developed in chapter 3, an equivalent source distribution over the heart shall be used in a model to model adjustment. This source distribution is known as the equivalent double layer. The double layer shall be estimated from simulated skin potentials. The results of this simulation shall be discussed in chapter 4.

As these results appear to be satisfactorily, finally the epicardial potentials shall be estimated from measured skin potentials in chapter 5.

---

## 2. PHYSICAL MODELLING OF THE HUMAN BODY AND THE DISPLAY OF THE DATA

### 2.1. The physical model of the human body.

In this study heart potentials shall be estimated from a set measured or simulated skin potentials. To make this calculation not too complicated and still keep the essence, the following assumptions are made:

- The human body is, as far as the electric fields are concerned, linear, homogeneous and isotropic. These properties have been suggested by Plonsey [4]. This assumption will only have influence on the heart-to-skin transfer function.
- The influence of the body-extremities (head, arms, legs) is neglected. This is allowed, because hardly any current will enter these extremities, as the torso resistancy is sufficiently low.
- The electric fields are supposed to be quasi-stationary, which is proved by Plonsey [4].
- The heart is approximated by a sphere, which encloses the heart tightly and which has a radius of about 70 mm. This assumption also has only influence on the heart-to-skin transfer function.
- The body and heart sphere are approximated by a limited number of flat triangles.
- The potential distribution is linear over these triangles.
- The heart does not move during the QRS-complex. This assumption appears to be realistic in practice.

In order to calculate the heart potentials, the geometry of the human body should also be known. Therefor and for the measurement of the skin potentials, arrangements are necessary about a point distribution on the torso and on the heart.

### 2.2. Definition of a point distribution on the torso and on the heart.

Some conditions are attached to the distribution of the measuring points on the torso. The number of measuring points shall be limited, due to:

- the size of the measuring electrodes;
- the grid of mutual independance of the skin potentials.

This point distribution ought to be so, that the density decreases as the distance to the heart increases. This is due to the fact, that close to the heart the potentials show higher spatial frequencies and are more reliable than at greater distance from the heart.

A point distribution, which satisfies these conditions, is designed by Damen [14] and further developed by Nicola [20]. This point distribution is obtained in the following way:



Choose the origin of a Cartesian coordinate system in the centre of the heart, i.e. roughly from the lower end of the sternum: 4 cm upwards, 3 cm to the left shoulder and 7 cm backwards (the axes are defined in figure 2). Define an octahedron, of which the centre coincides with the origin and the angular points lie on the axes. On the edges of the octahedron points are chosen in such a way, that these points divide the edges in  $NO$  equal parts. These points are connected with each other in such a way, that in each triangle of the octahedron  $NO^2$  congruent triangles appear ( see figure 1 ).

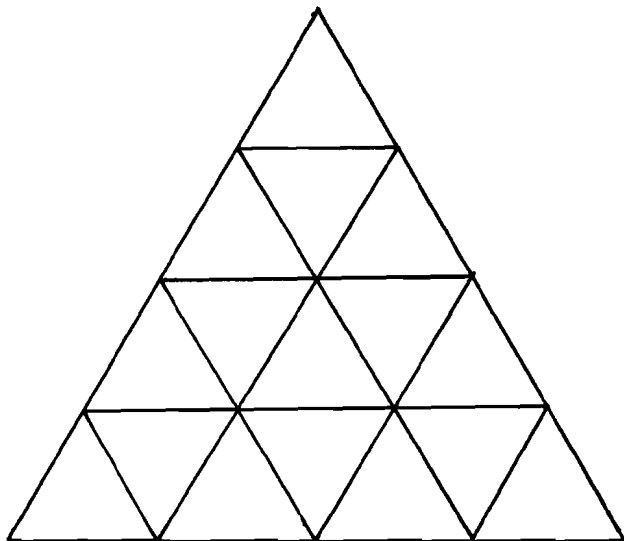


Fig. 1

Division of a triangle in  $NO^2$  congruent triangles (  $NO=4$  ).

So, over the whole octahedron appear  $8NO^2$  congruent triangles and  $4NO^2+2$  angular points. Next the octahedron will be "blown up", so that the angular points will be found on a sphere around the origin. So, in spherical coordinates the  $\theta$ - and  $\varphi$ -coordinate of an angular point are fixed. ( For more details see Nicola [20] ).

The measuring points on the torso are now those points, where the line, which connects an angular point with the origin, cuts through the torso surface. In this way a point distribution is made over the torso, as represented in figure 2.

The distance of a measuring point on the skin to the origin can be determined with a dedicated apparatus, as shown in figure 3.

The point distribution over the heart sphere is obtained in the same way, as is described before, with the help of an similar octahedron. The division of an edge of the octahedron in a number of equal parts, however, is denoted here by  $NH$  (  $NH \leq NO$  ).

The numbering of the angular points is defined spirally from top to bottom. In figure 4, this numbering is indicated for a part of the heart sphere.

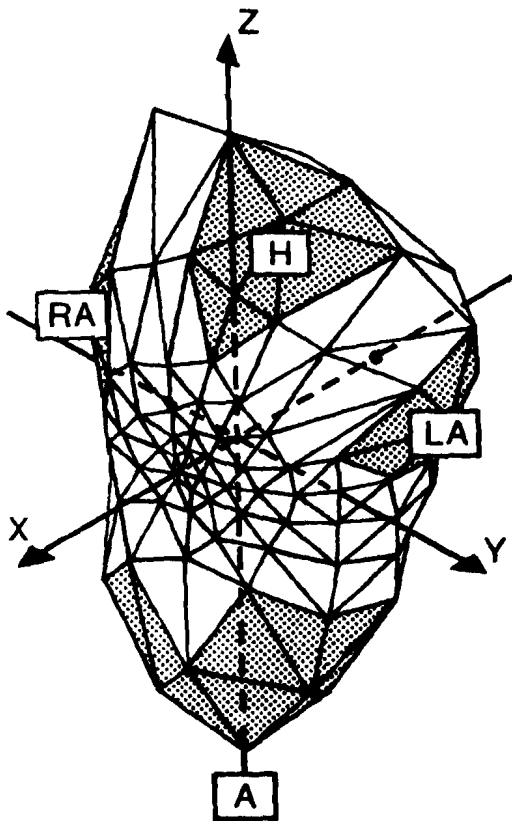


Fig. 2

The truncated torso approximated by 200 triangles.

H = Head side

RA = Right Arm side

LA = Left Arm side

A = Abdomen

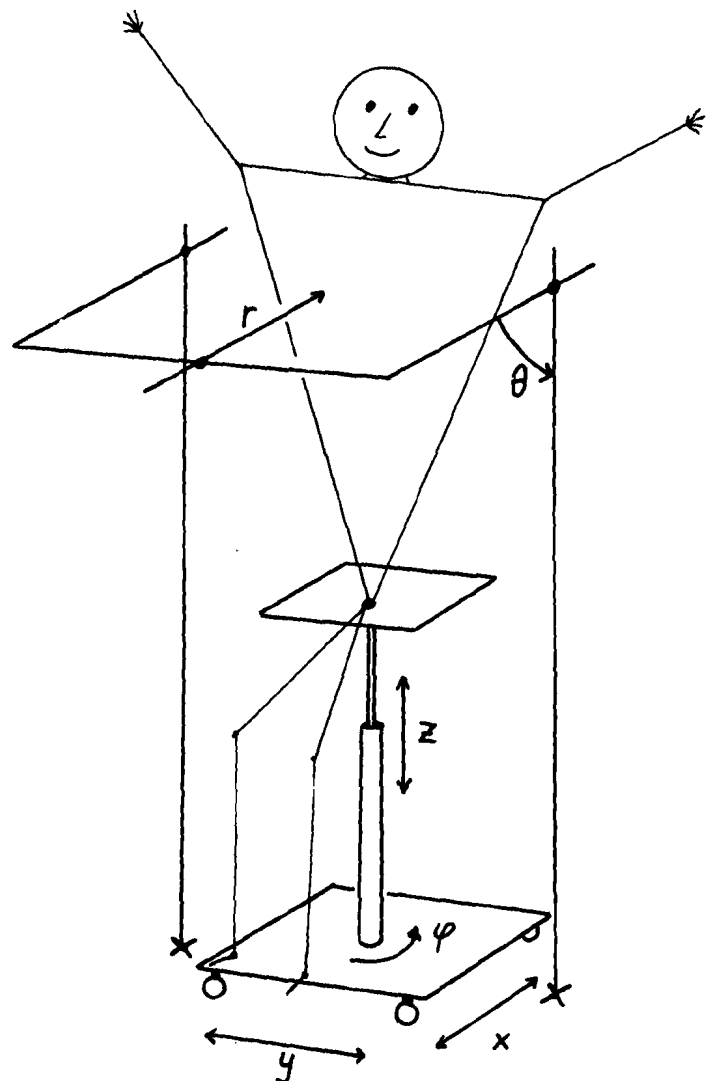


Fig. 3

Apparatus to measure the torso geometry. Provisions are made to position the heart centre in the origin of the coordinate system.

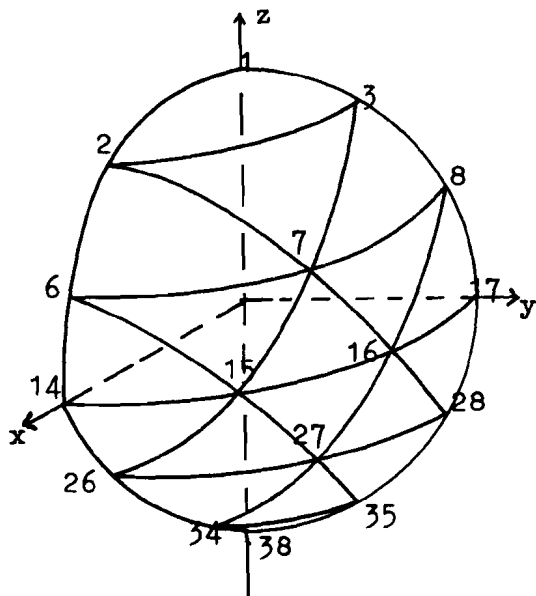


Fig. 4 Example of the point distribution on the heart sphere.  
(  $NH=3$  )

### 2.3. Presentation of the potentials on a closed surface

To visualise, for example, the calculated epicardial potentials on the heartsphere, a flat two dimensional projection of the three dimensional curved heartsphere - surface is necessary, likewise the necessity of a flat two dimensional projection of the torso exists. A projection method is used, which starts from the already used octahedron with a pointdistribution as described in paragraph 1.2. The edges at the back of this octahedron are opened and the four posterior triangles are unfolded until they lie in the same plane as their adjacent triangles. Next the angular points will be projected on a square in the y-z plane; in other words an observer in  $x = \infty$ .

This projectionmethod is represented once more in figure 5.

The projections of the torso surface and the heart surface are represented in figure 6 , where the pointdistributions are also placed. It should be remarked hereby, that the heart slightly reclines in the body, so that the atria point to the back of the body.

---

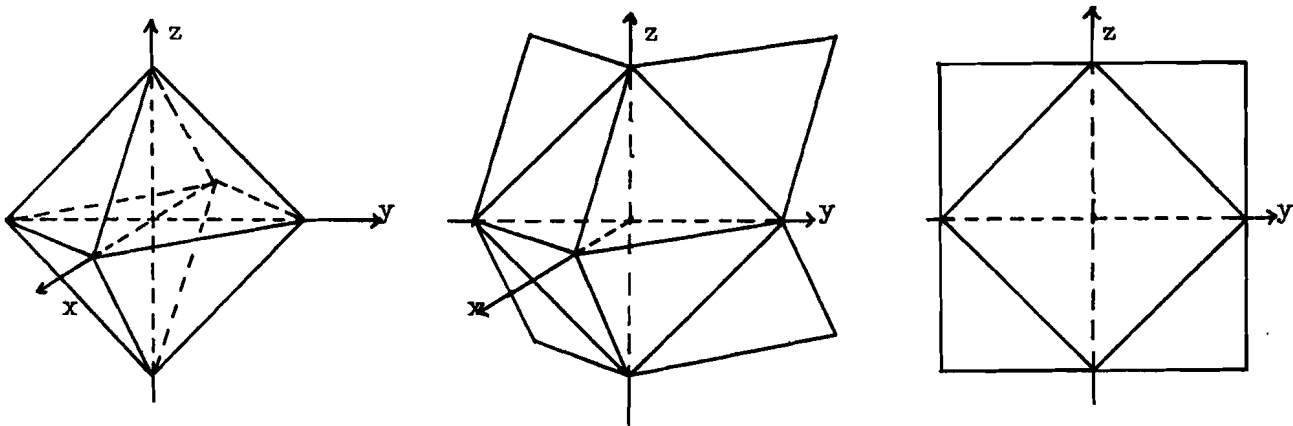


Fig. 5 A two-dimensional projection method.

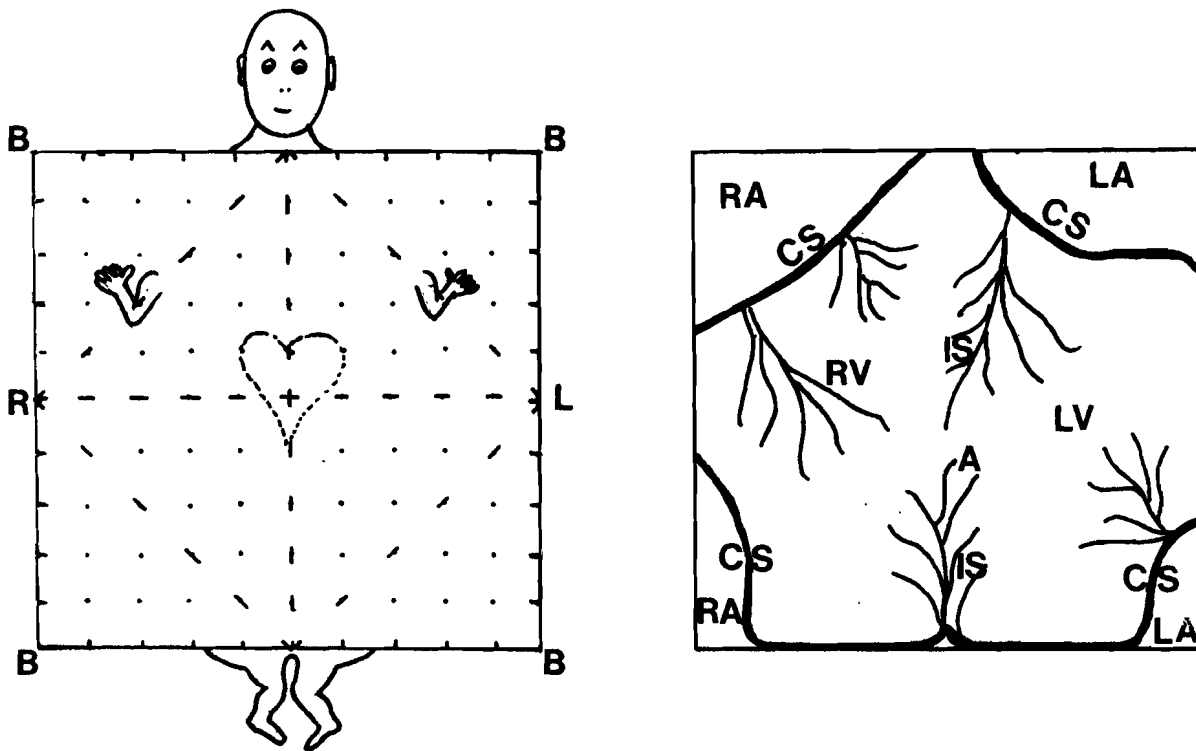


Fig. 6 Projections of the torso surface and epicardial surface.  
( NO=5 )

B = Backside  
L = Left side  
R = Right side

CS = Coronary Sulcus  
IS = Interventricular Sulcus  
LA = Left Atrium  
LV = Left Ventricle  
RA = Right Atrium  
RV = Right Ventricle

### 3. MATHEMATICAL DESCRIPTION OF THE PROBLEM

#### 3.1. Introduction of the Singular Value Decomposition (S.V.D.).

Any  $m \times n$  - matrix  $A$  with rank  $r$  can be decomposed with the help of the S.V.D. in :

$$A = U Q V^T \quad (1)$$

where :  $U$  is a leftunitary  $m \times r$  - matrix, so  $U^T U = I_r$  ;

$V$  is a leftunitary  $n \times r$  - matrix, so  $V^T V = I_r$  ;

$Q$  is a  $r \times r$  - diagonal matrix:

$$Q = \text{diag}(\sigma_1, \sigma_2, \dots, \sigma_r)$$

and  $\sigma_1 \geq \sigma_2 \geq \dots \geq \sigma_r > 0$ .

The  $\sigma_j$  's are known as the singular values.

Some properties of the S.V.D. will be used in this report; namely, if the S.V.D. of matrix  $A$  is given by (1), then:

- the pseudo - inverse  $A^+$  of  $A$  is:

$$A^+ = V Q^{-1} U^T \quad (2)$$

and the singular values of  $A^+$  are:  $\sigma_1^{-1}, \sigma_2^{-1}, \dots, \sigma_r^{-1}$  .

- the transposed matrix  $A^T$  of  $A$  is:

$$A^T = V Q U^T$$

- the norm of the matrix  $A$  is:

$$\begin{aligned} |A|^2 &= \\ &= \text{trace} ( A^T A ) = \text{trace} ( V Q^2 V^T ) \\ &= \text{trace} ( Q^2 ) = \sum_{j=1}^r \sigma_j^2 \end{aligned} \quad (3)$$

For more details about the S.V.D. is referred to the literature [21,19]

#### 3.2. The S.V.D. applied to the heart - to - skin transfermatrix.

With the suppositions that the human body is linear, homogeneous and isotropic, as far as the electric fields are concerned and that the electrical heart activity produces a quasi - stationary field, the transfermatrix from epicardial potentials to skin potentials can be proposed by a matrix, so that:

$$\phi_{ts} = A \phi_e \quad (4)$$

where :  $\phi_s$  is a vector, consisting of m elements,  
 namely the potentials in m points on the skin;  
 $\phi_e$  is a vector, consisting of n elements,  
 namely the potentials in n points on the heart,  $n \leq m$ ;  
 A is a mxn - transfermatrix.

On this transfermatrix one can apply the S.V.D. This S.V.D. of the transfermatrix A, given by (1), and substituted in(4) gives:

$$\phi_s = U Q V^T \phi_e \quad (5)$$

Each element  $\chi_{ej}$  of the vector  $\chi_e = V^T \phi_e$  can be considered as a projection of the vector  $\phi_e$  on the concerned column  $v_j$  of the matrix V ( see [21] ). So the columns of V can be interpreted as fundamental independant potential distributions over the heart sphere.

The potential distribution over the torso as a result of one such a fundamental potential distribution  $v_j$  over the heart , will be, because of the orthonormality of the columns of the matrix V, as follows:

$$\phi_s = U Q V^T v_j = \sigma_j u_j$$

So the orthonormal potential distributions over the heart lead, via the transfercoefficients  $\sigma_j$ , to orthonormal potential distributions over the skin surface.

Because of the fact that the singular values are ordered according to diminishing magnitude and because of the orthonormality of the columns of the matrix U, the "first" fundamental potential distributions over the heart will have a larger influence on the skin potentials than the "last" ones. The observability of a potential distribution over the heart on the skin is therefore so much the better as the singular value, belonging to the concerning potential distribution, is larger.

Starting with equation (4), it should be possible, in principle, to calculate the epicardial potentials out of a set measured skin potentials and a calculated matrix A, with:

$$\phi_e = A^+ \phi_s \quad (6)$$

where  $A^+$  is the pseudo - inverse of the matrix A. Is the S.V.D. of the matrix A given by (1), then the pseudo - inverse of A can be written as:

$$A^+ = V Q^{-1} U^T \quad (2)$$

Substitution of (2) in (6) gives:

$$\phi_e = V Q^{-1} U^T \phi_s \quad (7)$$

Each element  $\chi_{sj}$  of the vector  $\chi_s = U^T \phi_s$  is now to be regarded as a

projection of  $\phi_s$  on the concerned column  $u_j$  of the matrix U. The columns of U can thus be interpreted as fundamental independent potential distributions over the torso. The epicardial potential as a result of one such a fundamental potential distribution over the torso  $u_j$  is, because of the orthonormality of the columns of U, equal to:

$$\phi_e = V Q^{-1} U^T u_j = \sigma_j^{-1} v_j \quad (8)$$

So here the orthonormal potential distributions over the torso lead via the transfercoefficients  $\sigma_j^{-1}$  to orthonormal potential distributions over the heart.

If there was no noise on the skin potentials, the epicardial potentials could be calculated in this way. The influence of this noise will be discussed in the next paragraph.

### 3.3. The influence of the noise in the skin potentials.

In the last paragraph it has been proved, that a fundamental potential distribution  $v_j$  on the heart leads, via the transfer-coefficient  $\sigma_j$ , to a potentialdistribution  $\sigma_j u_j$  on the skin surface. If these  $v_j$ 's have an equal chance of occurrence, then all the distributions  $\sigma_j u_j$  will equally occur in the skin potentials. However, the ratio between the largest and the smallest singular value is a factor 10.000 ( see figure 18), while the skin potentials can be measured with a maximal signal to noise ratio of about 50 dB, which equals a factor 300 ( see [15] ). This means, that the components of the skin potentials, corresponding to the smallest singular values, can never be measured, because the noise will extremely corrupt these potentials. Consequently this means, that the epicardial potentials cannot be calculated accurately.

If  $\phi_b$  is a vector, consisting of the real skin potentials corrupted by noise, then this vector can be analysed in a noise-free component  $\phi_s$  and a noisevector  $\xi$ , so that:

$$\phi_b = \phi_s + \xi \quad (9)$$

One may suppose, that the noise in the processed skin potentials is white, so that:

$$E[\xi] = 0 ; \quad E[\xi \cdot \xi^T] = s^2 I ; \quad E[\phi_s \cdot \xi^T] = 0 ;$$

where E stands for expectation and s for the standard deviation and I is the identity matrix.

Substitution of equation (5) in (9) and multiplication with  $U^T$  gives:

$$U^T \phi_b = Q V^T \phi_e + U^T \xi$$

or: 
$$y = Q w + v \quad (10)$$

where the vectors  $\underline{y}$  and  $\underline{w}$  contain respectively the orthonormal potential distributions on the skin and on the heart. Calculating inversely the vector  $\underline{w}$ , with the help of a least squares method, gives:

$$\hat{\underline{w}} = Q^{-1} \underline{y} = \underline{w} + Q^{-1} \underline{v}$$

and from this it follows:

$$E[(\hat{\underline{w}} - \underline{w})(\hat{\underline{w}} - \underline{w})^T] = s^2 Q^{-2}$$

So the signal to noise ratio for a potential distribution  $w_j$  on the heart will become worse, if the corresponding singular value  $\sigma_j$  decreases. In other words, the pattern of  $w_j$  will become unrecognizable if:

$$\frac{E[(\hat{w}_j - w_j)^2]}{E[w_j^2]} > 1$$

This inequality will hold especially for the badly observable potential distributions on the posterior part of the epicard, while the distributions on the anterior epicard correspond to the greatest singular values and consequently have a good signal to noise ratio.

Before passing on to further conclusions we have to make a clear insight into the signal to noise ratio of the skin potentials. Therefore it is necessary that ergodicity is supposed. Then it is possible to make an estimation of the covariance of  $\underline{y}$ , namely:

$$\Psi_{yy} = E[\underline{y} \cdot \underline{y}^T] = \lim_{T} \frac{1}{T} \int_0^T \underline{y} \cdot \underline{y}^T dt$$

If the vector  $\underline{y}$  is discretised in time, then the vector  $\underline{y}$  will be changed into a matrix  $Y$ , as will be discussed on page 19. A row of  $Y$  then gives one fundamental potential distribution over the skin as a function of the time and a column of  $Y$  contains the fundamental skin potential distributions at one point of time as a function of the serial number of these distributions.

On this matrix  $Y$  one can apply the S.V.D., so that:

$$Y = K L M^T$$

The estimation of the covariance of  $\underline{y}$  can be written now as:

$$\Psi_{yy} = K L^2 K^T \quad (11)$$

A rough approximation can be made by the simplification, that all fundamental potential distributions  $v_j$  on the heart have an equal chance of occurrence and no interdependence.\* This means in formula:

$$E \underline{w} \cdot \underline{w}^T = c^2 I \quad (12)$$

---

\*Lateron ( see page 34 ) this assumption appears to be unrealistic, but the derived limit seems to be appropriate.



An indication about the value of  $c$  can be obtained from the equations (10), (11) and (12). Namely:

$$E[\underline{y} \cdot \underline{y}^T] = \sum l_j^2 = c^2 \sum \sigma_j^2 + \sum s^2$$

where  $l_j$  is a singular value of the matrix  $Y$ .

As  $s^2$  can be estimated from the signal to noise ratio of the ECG's and the singular values  $l_j$  and  $\sigma_j$  are known, the constant  $c^2$  will be:

$$c^2 = \frac{\sum l_j^2 - \sum s^2}{\sum \sigma_j^2}$$

From  $y_j = \sigma_j w_j + v_j$  and (12) can be concluded, that a potential distribution  $w_j$  can be estimated reliably if  $c \sigma_j^2 > s^2$ , because then the signal to noise ratio will be approximately greater than 1. Suppose that only  $k$  of these distributions can be estimated reliably, i.e. a signal to noise ratio greater than 1, then the estimation of the remaining potential distributions will make no sense, because these distributions will be strongly corrupted by noise.

Now the conclusion is, that in the inverse calculation of the epicardial potentials from the skin potentials, the small singular values  $\sigma_j$ , that are the singular values with a relative large  $j$ , will lead to large errors in the epicardial potentials, because of the noise in the skin potentials.

These errors can be reduced by setting the inverse singular values, belonging to the distributions, which lie below the noise level, equal to zero; so:

$$\sigma_{k+1}^{-1} = \sigma_{k+2}^{-1} = \dots = \sigma_r^{-1} = 0$$

So the epicardial potentials can be approximated by:

$$\hat{\phi}_{e1} = V_1 Q_1^{-1} U_1^T \phi_b \quad (13)$$

where :  $V_1$  is a leftunitary  $n \times k$  - matrix, containing the first  $k$  columns of the matrix  $V$ ;

$U_1$  is a leftunitary  $m \times k$  - matrix, containing the first  $k$  columns of the matrix  $U$ ;

$Q_1^{-1}$  is a  $k \times k$  - diagonal matrix, containing the first  $k$  diagonal elements of the matrix  $Q^{-1}$ ; so:

$$Q_1^{-1} = \text{diag}(\sigma_1^{-1}, \sigma_2^{-1}, \dots, \sigma_k^{-1})$$

Consequently the error, because of the noise, will be:

$$\Delta \hat{\phi}_{e1} = V_1 Q_1^{-1} U_1^T \xi$$

Another error exists, because a part of the epicardial potentials  $\phi_e$  is not estimated from the skin potentials. Namely the real epicardial potentials are:

$$\begin{aligned} \phi_e &= V Q^{-1} U^T \phi_s \\ &= \hat{\phi}_{e1} - \Delta \hat{\phi}_{e1} + V_2 Q_2^{-1} U_2^T \phi_s \end{aligned} \quad (14)$$

where :  $V_2$  is a left unitary  $n \times (n-k)$  - matrix, containing the last  $(n-k)$  columns of the matrix  $V$ ;

$U_2$  is a left unitary  $m \times (n-k)$  - matrix, containing the last  $(n-k)$  columns of the matrix  $U$ ;

$Q_2^{-1}$  is a  $(n-k) \times (n-k)$  - diagonal matrix, containing the last  $(n-k)$  diagonal elements of the diagonal matrix  $Q^{-1}$ ; so:

$$Q_2^{-1} = \text{diag}(\sigma_{k+1}^{-1}, \sigma_{k+2}^{-1}, \dots, \sigma_r^{-1})$$

The vector  $\underline{x} = Q_2^{-1} U_2^T \underline{\phi}_g$  cannot be determined on the basis of the skin potentials, because of the bad signal to noise ratio. Nevertheless, the vector  $\underline{x}$  indicates exactly the number of remaining degrees of freedom and it can be used to estimate the real epicardial potentials, with the help of the a priori information about the electrical heart activity, so that:

$$\hat{\underline{\phi}}_e = V_1 Q_1^{-1} U_1^T \underline{\phi}_b + V_2 \underline{x} \quad (15)$$

where  $\hat{\underline{\phi}}_e$  is the estimated epicardial potential.

Finally it should be remarked, that the vector  $\underline{x}$  may not exceed a certain amplitude limit, as in that case the contribution of  $\underline{x}$  would exceed the noise level. And this was the criterion to omit  $\underline{x}$ . After the vector  $\underline{x}$  is estimated, it turned out that  $\underline{x}$  did not exceed this limit, so that it was not necessary to take any precautions.

#### 3.4. The estimation of the epicardial potentials with the help of the a priori information.

In paragraph 3.3. it appeared, that it should be possible to estimate the epicardial potentials better with the help of the a priori information about the electric heart activity. This a priori information consists among other things of the following approximations:

- 1) The electric heart activity during the QRS-complex is almost exclusively determined by the depolarisation of both ventricles; so, both atria can be regarded as inactive.
- 2) For a healthy heart holds, that per cyclus each area of the heart muscle depolarises and that this depolarisation is unique per cyclus.
- 3) The polarity of the potential difference over the heart wall is fixed during the depolarisation; namely the outside is positive with regard to the inside and the amplitude is constant.
- 4) The depolarisation is a wave-phenomenon, which extends, as far as the ventricles are concerned, roughly from the apex over the whole of the heart surface and finally ends on the atrio-ventricular septum.

These conditions, except for the last one, are realised in a so-called "ON-OFF" model ( see [5,18] ); namely:

- ad 1+2) It is supposed, that only the ventricles are active during the QRS-complex and that each area of the heart depolarises only once per cyclus.  
That only the ventricles depolarize during the QRS-complex, can be realised with a socalled "depolarisation-demand". This demand indicates for each area on the ventricles, that it should have at least one moment, on which the area is electrically active.  
If an area of the heart has been depolarised, then, if the heart muscle is not fibrillating, that area will not depolarize once more in the same cycle.
- ad 3) It is also supposed, that during the depolarisation the outside of the heart wall is positive with regard to the inside and that the amplitude of the potential difference over the heart wall is constant. This supposition is made because of the fact that an active cellmembrane can be represented by current double layer. The electrical activity of a heart muscle cell can be replaced by a current dipole with strenght  $\mathcal{C}$ , per surface area and this double layer strenght is directly proportional to the transmembrane potential. ( For more details is referred to the literature [4,12] )  
Because this double layer has an obvious on-off character, this is the reason why an "ON-OFF" model is choosen.  
In the beginning this model only holds for the equivalent double layer, but in this report shall be supposed that it will also hold for the epicardial potentials.
- ad 4) The supposition about the wave-phenomenon is not used in this model, because the other demands are probably sufficient to obtain reliable epicardial potentials and the wave-phenomenon is automatically satisfied. As will turn out later ( see page 26 ), the epicardial potentials could probably have been estimated better in special parts of the epicard, if a demand about the wave-phenomenon was present.  
Still this demand is not used, because at the same time the chance exists, that a possible heart defect will be excluded, if too many demands are taken into account.

On the basis of these conditions, the epicardial potentials can be proposed by:

$$\tilde{\phi}_e = b \cdot \underline{z} \quad (16)$$

where : b is a constant;

$\underline{z}$  is a binary vector, i.e. consisting of discrete functions of the time, which only can have the values 0 or 1.

In order to derive more realistic epicardial potentials we have to estimate the vector  $\underline{x}$  in equation (15) in such a way, that the finally estimated epicardial potentials  $\phi_e$  satisfy the conditions. In other words, we would like that these estimated epicardial potentials are equal to the epicardial potentials in equation (16). It is obvious, that the processed method is not the only solution

for this problem, but as will turn out later, this method will lead to satisfactory results.

That the estimated epicardial potentials from equation (15) equals the epicardial potentials in (16) can be achieved with the help of a least squares method. The constant  $b$  and the vectors  $\underline{x}$  and  $\underline{z}$  are to be estimated now in such a way, that the following criterion is minimal:

$$E = \int \| \hat{\phi}_{e1} + V_2 \underline{x} - b \cdot \underline{z} \|^2 dt \quad (17)$$

Therefore the parameter  $b$  is to be chosen, so that:

$$\frac{\partial E}{\partial b} = 0$$

From this follows for the constant  $b$ :

$$b = \frac{\int \underline{z}^T (\hat{\phi}_{e1} + V_2 \underline{x}) dt}{\int (\underline{z}^T \cdot \underline{z}) dt} \quad (18)$$

If  $\underline{x}(t)$  per moment is chosen in such a way, that the contribution in (17) is minimal, then the error  $E$  will also be minimal.  
From:

$$\frac{\partial}{\partial \underline{x}} \| \hat{\phi}_{e1} + V_2 \underline{x} - b \cdot \underline{z} \|^2 = 0$$

follows the trivial relation:

$$\underline{x} = V_2^T [b \cdot \underline{z} - \hat{\phi}_{e1}] \quad (19)$$

Substitution of this equation in (17) and (18) gives:

$$b = \frac{\int \underline{z}^T [I - V_2 V_2^T] \hat{\phi}_{e1} dt}{\int \underline{z}^T [I - V_2 V_2^T] \underline{z} dt} \quad (20)$$

$$E = \int \| [I - V_2 V_2^T] [\hat{\phi}_{e1} - b \cdot \underline{z}] \|^2 dt \quad (21)$$

Notice that the equation for the constant  $b$  can be regarded as the quotient of a cross-correlation and an auto-correlation.

Before passing on to further calculations, the vectors  $\hat{\phi}_{e1}$ ,  $\underline{z}$  and  $\underline{x}$  are discretised in time. The vectors  $\hat{\phi}_{e1}$ ,  $\underline{z}$  and  $\underline{x}$  will be changed into respectively the pxt-matrices POTH and Z and a dxt-matrix X. The character  $p$  stands for the number of positions on the heart and  $t$  stands for the number of points in time, on which a sample is taken. The character  $d$  stands for the number of degrees of freedom left.

So, for example, a row of POTH gives the calculated epicardial potential at one point on the heart as a function of the time and a column of POTH gives the potentials at one point of time as a function of the serial number of the points on the heart.

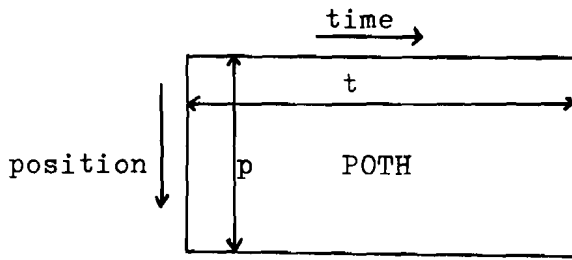


Fig. 7 Dimensions of the matrix POTH.

In the discretised situation the equations (19) until (21) become respectively:

$$X = V_2^T [ bZ - POTH ] \quad (22)$$

$$b = \frac{ZTCP}{ZTCZ} \quad (23)$$

$$E = PTCP + b^2 ZTCZ - 2bZTCP \quad (24)$$

where :  $PTCP = \text{trace}( POTH^T [ I - V_2 V_2^T ] POTH )$

$$ZTCP = \text{trace}( Z^T [ I - V_2 V_2^T ] POTH )$$

$$ZTCZ = \text{trace}( Z^T [ I - V_2 V_2^T ] Z )$$

So, if a matrix Z is given, then it is possible to calculate with this Z, together with a known matrix POTH, the error E.

The estimation of the epicardial potentials is an iterative procedure. During each iteration cycle a check is made in each angular point, whether an one element extension or shortening of an interval where  $Z[p,t] = 1$ , results in a smaller error E. If this is the case, then the new value of E will be adopted, while the old value will be maintained, if the new error is larger. If in every angular point no more changes occur, the iteration process will be stopped. The present matrix Z, together with the constant b, then will form an estimation of the depolarisation-wave on the heart.

#### 4. ESTIMATION OF THE EQUIVALENT DOUBLE LAYER FROM SIMULATED SKIN POTENTIALS

Instead of the epicardial potentials often the so-called equivalent double layer strength  $\tau$  is calculated. This equivalent double layer is briefly mentioned already in paragraph 3.4.

In this chapter the equivalent double layer will be estimated from simulated skin potentials, which are mathematically obtained from an artificial double layer on the heart surface. So, in this way we have a method to test the theory developed in chapter 3.

But firstly some remarks shall be necessary with respect to the artificial double layer and to the transfermatrix, which relates this double layer with skin potentials.

##### 4.1. The artificial double layer on the heart surface.

In order to calculate skin potentials from which a double layer will be estimated, it is necessary, that a physically possible double layer as a function of the time is known.

Such a double layer is suggested per cycle in the so-called "String Model" ( see [10] ). The propagation of this double layer proceeds smoothly over the heart surface with a constant amplitude, as is represented in Annex 1.

In the String Model the heart is approximated again by a sphere as described in chapter 2. The heart is divided into four compartments, namely the both atria and the both ventricles. The heart wall is supposed to be infinitely thin and the atrio-ventricular septum is proposed by a flat plane.

The artificial double layer will only be active in the area of the ventricles. A profile of this model is represented in figure 8.

The position of the double layer on a fixed moment is also represented in this profile.

The double layer on the heart surface lies between the boundaries ( in spherical coordinates ):

- i)  $\theta_{lmin}$  and  $\theta_{lmax}$  in the left ventricle;
- ii)  $\theta_{rmin}$  and  $\theta_{rmax}$  in the right ventricle.

These boundaries move in time according to the formula:

$$\theta(t) = \frac{\pi}{2} \pm \frac{Ve}{R}( t - t_1 )$$

where :  $Ve$  = propagation speed in the Purkinje fibres ( ca. 2 mm/sec );

$R$  = radius of the heart sphere ( ca. 70 mm );

$t_1$  = time space between the endocardial start and the moment, on which the double layer reaches the epicardium;

$\pm$  : the plus sign in this formula concerns the right ventricle and the minus sign concerns the left ventricle.

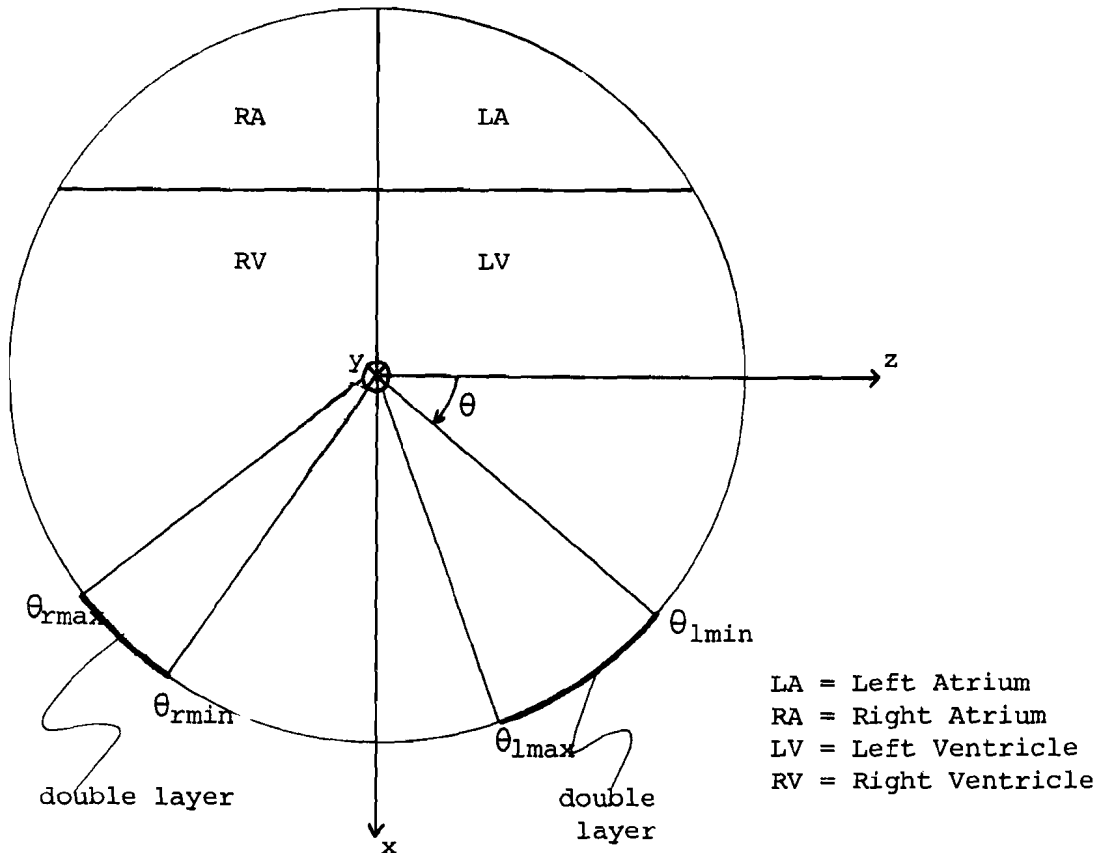


Fig. 8 Profile of the String Model

So each msec.  $\theta(t)$  progresses ca.  $2^\circ$ .  
 For the case that  $NH = 4$ , 16 points will lie on the diameter of the heart sphere, so that about 12 msec. pass, before the double layer reaches the following point on the heart surface. So, because of the rather coarse point distribution on the heart, the artificial double layer will not proceed continuously. In Annex 2 and 3 the side-views of respectively the left and right ventricle are represented, with under it the course of the artificial double layer in the different points on the heart as a function of the time. Hereby it should be remarked, that the points 9, 11, 57 and 59 lie exactly on the atrio-ventricular septum. The computer program, which calculates this artificial double layer, generates on special moments in the points 9 and 57 an activity of the double layer, but it does not so in the points 11 and 59. In this way an asymmetric source distribution will appear, but this will have no further consequences.

---

4.2. The transfermatrix relating double layer intensities to skin potentials.

In order to calculate the skin potentials from the simulated double layer, a relation should be known between this double layer and the skin potentials. With the help of the suppositions mentioned in paragraph 3.2., it is possible to introduce a transfer matrix from double layer to skin potentials, so that:

$$\underline{\phi}_s = E \underline{z}_e \quad (25)$$

where :  $\underline{\phi}_s$  is a vector, consisting of m elements,  
 namely the potentials in m points on the skin;  
 $\underline{z}_e$  is a vector, consisting of n elements,  
 namely the double layer activity in n points on the heart surface;  
 E is a mxn - transfermatrix (  $n \leq m$  ).

For more details about this transfermatrix is referred to the Appendix and to the literature [22].

On the matrix E one can apply the S.V.D., so that:

$$\underline{\phi}_s = U Q V^T \underline{z}_e \quad (26)$$

where : U and V are respectively leftunitary mxn- and nxn-matrices;  
 Q is a nxn-diagonal matrix, of which the last element is equal to zero ( see Appendix ); so:

$$Q = \text{diag}(\sigma_1, \sigma_2, \dots, \sigma_{n-1}, 0)$$

Though the denomination of these matrices is the same as in paragraph 3.4., it may be clear, that they are not identical.

Inversion of equation (26) gives:

$$\underline{z}_e = V Q_r^{-1} U^T \underline{\phi}_s \quad (27)$$

where  $Q_r^{-1}$  is the inverse of the diagonal matrix Q, with the restriction that the inverse of the last element of Q is defined equal to zero;  
 so:

$$Q_r^{-1} = \text{diag}(\sigma_1^{-1}, \sigma_2^{-1}, \dots, \sigma_{n-1}^{-1}, 0)$$

We are allowed to do so, because only the first k inverse singular values will be used in the inverse calculation of the equivalent double layer. This analogous to what is described in chapter 3 for the epicardial potentials.

It is also possible to estimate the equivalent double layer with the formula:

$$\hat{\underline{z}}_e = V_1 Q_1^{-1} U_1^T \underline{\phi}_b + V_2 \underline{x} \quad (28)$$



where :  $\hat{\underline{z}}$  is the estimated double layer and  $V_1, Q_1^{-1}, U_1^T, V_2, \phi_b$  and  $\underline{x}$  have a corresponding meaning as in equation (15).

#### 4.3. Estimation of the equivalent double layer.

In the last paragraph has been shown, that the equivalent double layer can be estimated with the help of equation (28). This equivalent double layer can be presented by the vector  $b.z$  ( see page 18), in which the constant  $b$  and the vector  $\underline{z}$  have the same signification as in equation (16).

Now the constant  $b$  and the vectors  $\underline{z}$  and  $\underline{x}$  are to be estimated in such a way, that the following criterion is minimal:

$$E = \int \| \hat{\underline{z}}_{e1} + V_2 \underline{x} - b.z \| ^2 dt \quad (29)$$

$$\text{where } \hat{\underline{z}}_{e1} = V_1 Q_1^{-1} U_1^T \phi_b \quad (29a)$$

The estimation of the equivalent double layer from equation (29) progresses completely analogous to the way in which the epicardial potentials are estimated from equation (17).

The only remaining problem is: howmany singular values should be taken into account in the estimation of the equivalent double layer. Namely in paragraph 3.3. is stated, that the epicardial potentials could be estimated better, if a number of inverse singular values are set to zero. Consequently the same will hold for the equivalent double layer. The number of inverse singular values, that should not be set to zero, can be calculated from the noise influence. For the calculation of this number is referred to the literature [21].

##### 4.3.a Results in noisefree case.

The simulated skin potentials in 102 points on the torso, from which the double layer will be calculated, are plotted in figure 9. The total enveloping square is the projection of the skin surface, as described in paragraph 2.3.

These skin potentials are calculated from equation (25), by which the simulated double layer on the heart surface was given in 66 points. The amplitude is choosen to be equal to 47.

The first step in the estimation of the equivalent double layer will be the calculation of the relatively well observable part of this double layer  $\hat{\underline{z}}_{e1}$ , with the help of equation (29a). The number of inverse singular values, that are not set to zero, is equal to 35. This number is derived from the noise influence and is calculated from the data in paragraph 4.3.b. In this way we now have a possibility to compare the equivalent double layers, which are estimated from skin potentials with and without noise.

Before passing on to the iteration, as described in paragraph 3.4.,  $\hat{\underline{z}}_{e1}$  will be made non-negative. This on the ground of the a priori information which says, that during the depolarisation the outside of

the equivalent double layer is positive with respect to the inside ( see paragraph 3.4.). The iteration process will start on this non-negative  $\xi_{-e1}$ .

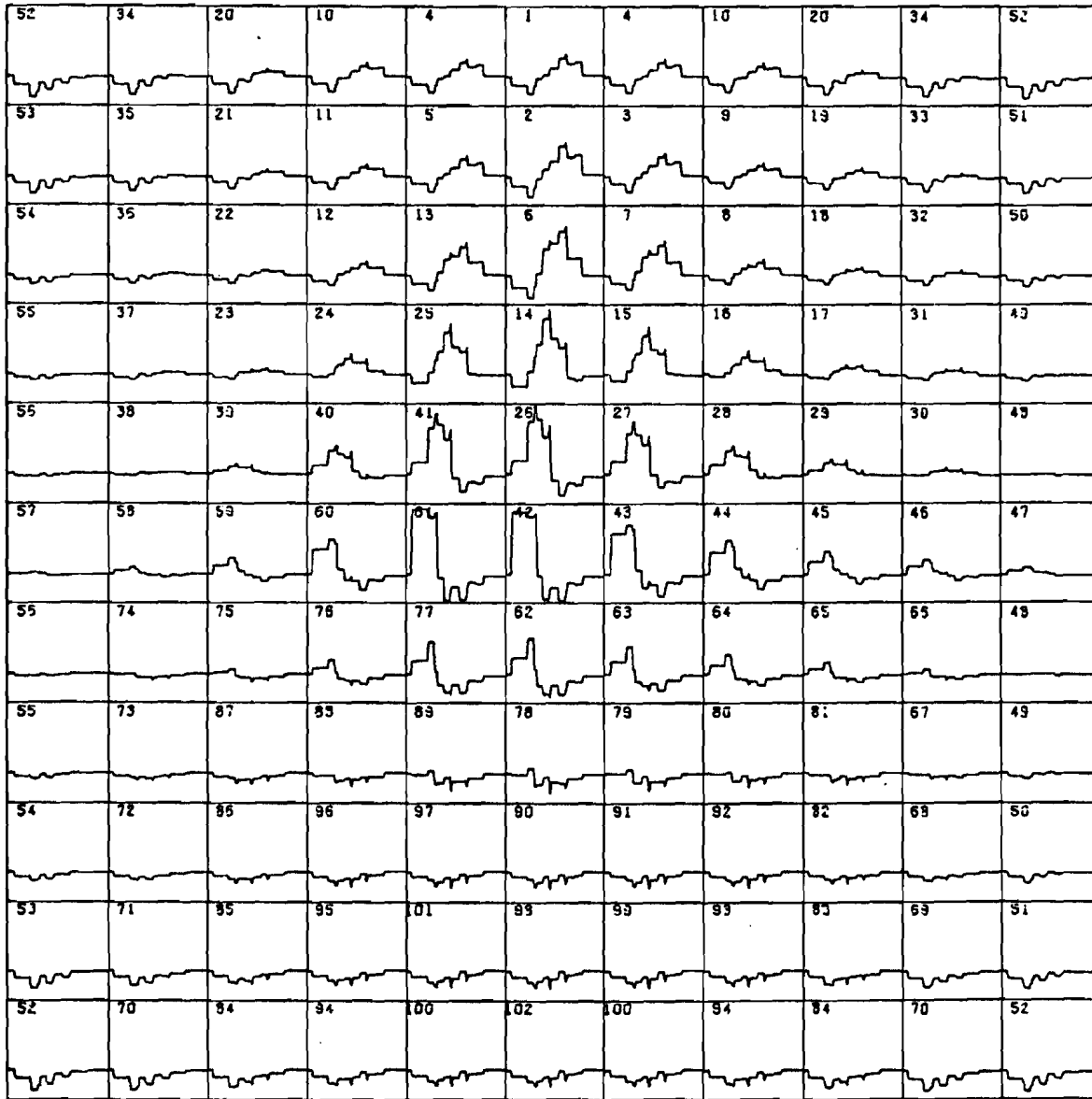


Fig. 9 The simulated skin potentials without noise.

The final results can be seen in figure 10, in which the estimated equivalent double layer in 66 points on the epicard has been plotted, together with the simulated double layer ( interrupted line ) and the vector  $b_z$  ( thin line ).

From this figure can be concluded, that the double layer is estimated pretty good, especially in the anterior region. Only in the points 57, 60 and 66 the estimation is bad. The reason of that is a wrong start

situation. By this is meant, that the moment of time, wherefor  $Z[p,t] = 1$  has been chosen before the iteration is started, does not lie in the interval, wherein the double layer ought to be. Because of the fact, that in these points ( and also in point 59 ) the estimated double layer only last for one point of time, it is obvious, that these estimations are based on a calculation error, i.e. a relative minimum of the error function has been reached. The bad estimation of the equivalent double layer in point 66 might have been anticipated, if there had been a demand for a wave-phenomenon ( see page 18). The estimation of the constant  $b$  is also very good, as can be seen in figure 10. It differs only 2% from the amplitude of the simulated double layer.

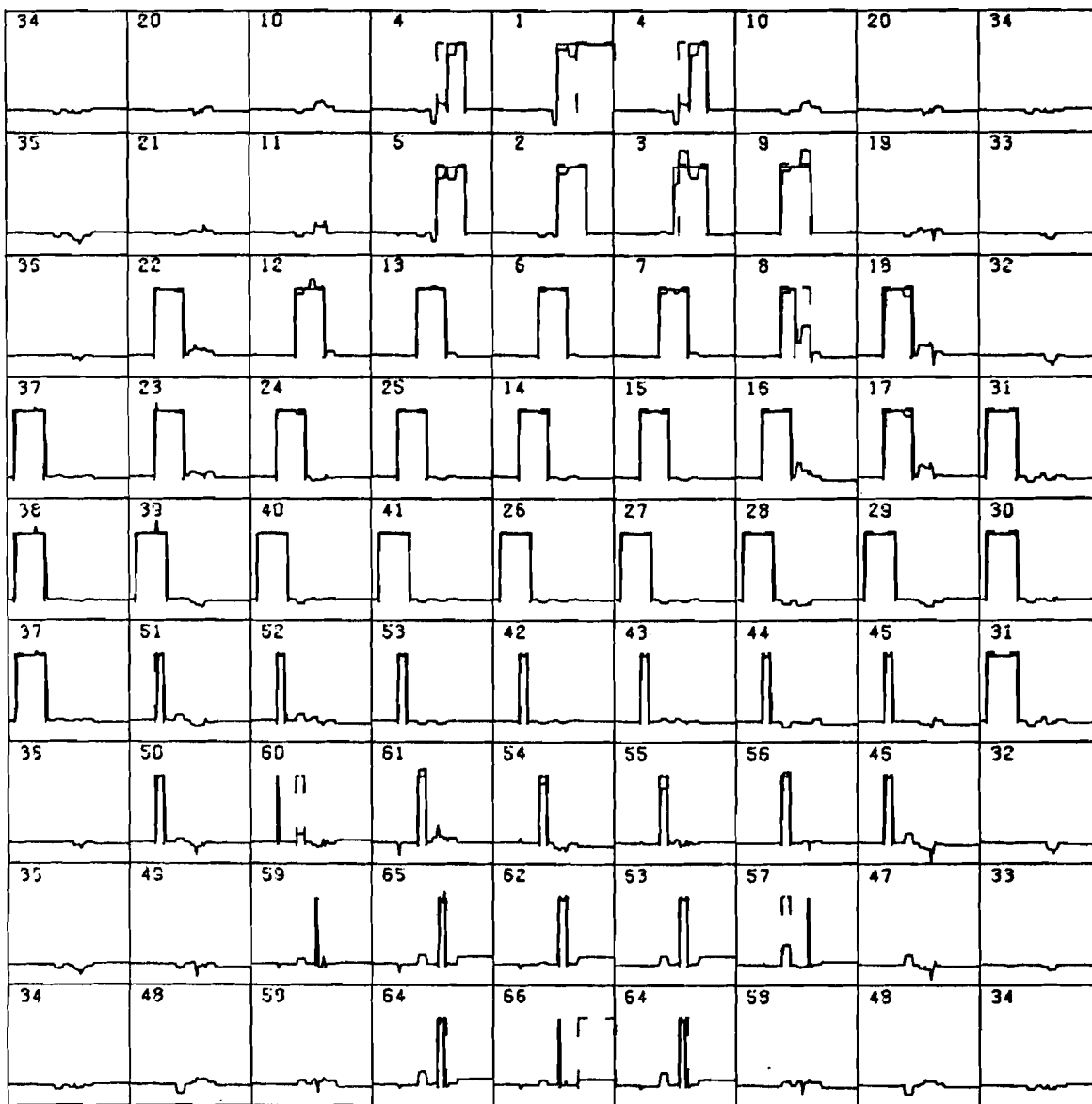


Fig. 10 Estimated double layer on the heart surface ( from simulated skin potentials without noise ), plus the simulated double layer (interrupted line) and the vector  $b.z$  (thin line).

If the estimated double layer  $\hat{\underline{z}}_e$  should be equal to the real double layer  $\underline{z}_e$ , then it can be derived that:

$$\underline{x} = V_2^T \hat{\underline{z}}_e = V_2^T \underline{z}_e$$

This equation can be found, when equation (28) is multiplied by  $V_2^T$ . The elements of the vector  $\underline{x}$  can now be regarded as the projections of the double layer on the columns of the matrix  $V$ .

In order to check this validity, the vector  $\underline{x}$  and the vector  $V_2^T \underline{z}_e$  are plotted in respectively Annex 4 and 5. It can be seen, that except for the last elements, both vectors show much resemblance.

The last element of the vector  $V_2^T \underline{z}_e$  is equal to the average double layer strength, because of the fact, that the last column of the matrix  $V$  is equal to the unit vector ( see Appendix ). The difference between the last element of the vector  $V_2^T \underline{z}_e$  and the last element of the vector  $\underline{x}$  is due to the fact that in the inverse calculation the relatively well observable part of the double layer,  $\underline{z}_{e1}$ , is made non-negative. By doing so, at each moment of time a constant is added to  $\underline{z}_{e1}$  and consequently this signal will find expression in the last element of the vector  $\underline{x}$ .

All in all the equivalent double layer can be estimated good, if no noise is present on the skin potentials.

#### 4.3.b Results in noisy case.

After the results from skin potentials without noise appeared to be satisfactorily, next the estimation algorithm shall be examined for the influence of the noise. Therefore some normally distributed noise  $\underline{\xi}$  will be added to the skin potentials in figure 9. From this noise is given that:

$$E[\underline{\xi}] = \underline{0} \quad ; \quad E[\underline{\xi} \cdot \underline{\xi}] = s^2 I$$

and  $s^2 = \frac{1}{100}$  ( arbitrary units )

The value of the variance of the noise has been derived from the literature ( see for example [9, 12, 15] ).

The skin potentials with noise, from which the equivalent double layer shall be estimated, are plotted in figure 11. This estimation is performed as described in paragraph 4.3.a. The number of inverse singular values, that should not be set equal to zero, has been calculated from the noise influence ( see [21] ). This number appears to be equal to 35, so that 31 inverse singular values of the transfer matrix from double layer to skin potentials are set equal to zero.

Again the estimated equivalent double layer, the simulated double layer ( interrupted line ) and the vector  $\underline{b.z}$  ( thin line ) are plotted in one figure ( see figure 12 ). In comparison with figure 10 can be stated that the estimated double layer now has a rather noisy character and by that generates "disturbance peaks" in the points 10, 19, 32, 33, 34, 36, 48 and 59. These points all lie in the posterior region of the heart, where the estimation algorithm has a greater freedom to determine the equivalent double layer. However in general the double layer is estimated pretty good, especially in the anterior

region. A bad estimation is only derived in the points 57, 60 and 66, for the same reason as described in paragraph 4.3.a and in the points 1, 4, 5, 9, 17, 22 and 65.

The constant  $b$  is also well estimated. Now it differs less than 1% from the amplitude of the simulated double layer.

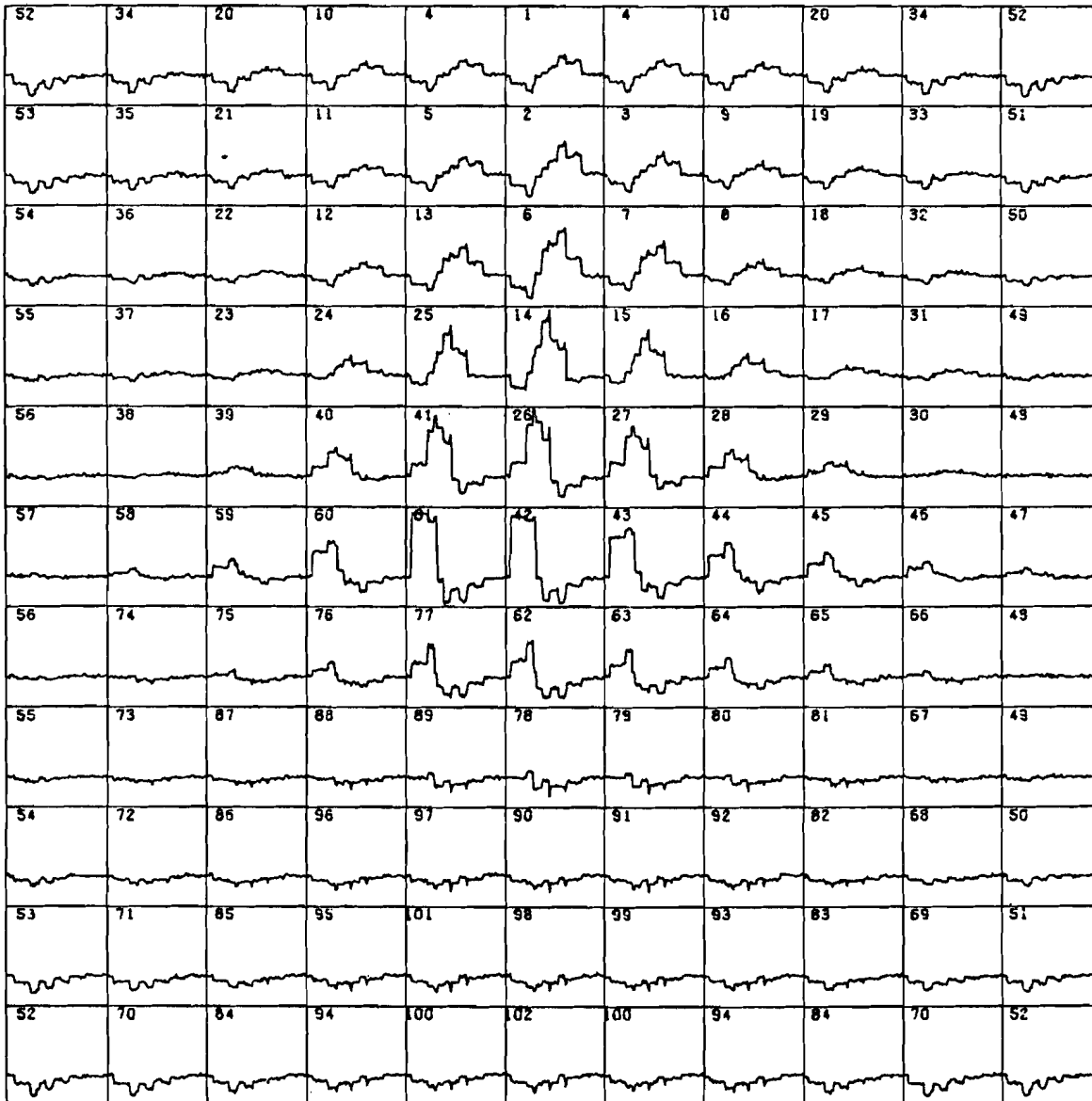


Fig. 11 The simulated skin potentials with noise.

The estimated vector  $x$  has been plotted in Annex 6. In comparison with the vector  $V_1 \hat{z}_e$  in Annex 5 can be seen, that these vectors show some resemblance, <sup>2</sup> except for the last element. That the last elements of these vectors can not be equal is explained on page 27, but in this case the last element of the vector  $x$  is also clearly corrupted by the noise. ( The sensivity of the vertical scale in Annex 6 is about the double from the sensivity in Annex 5. )

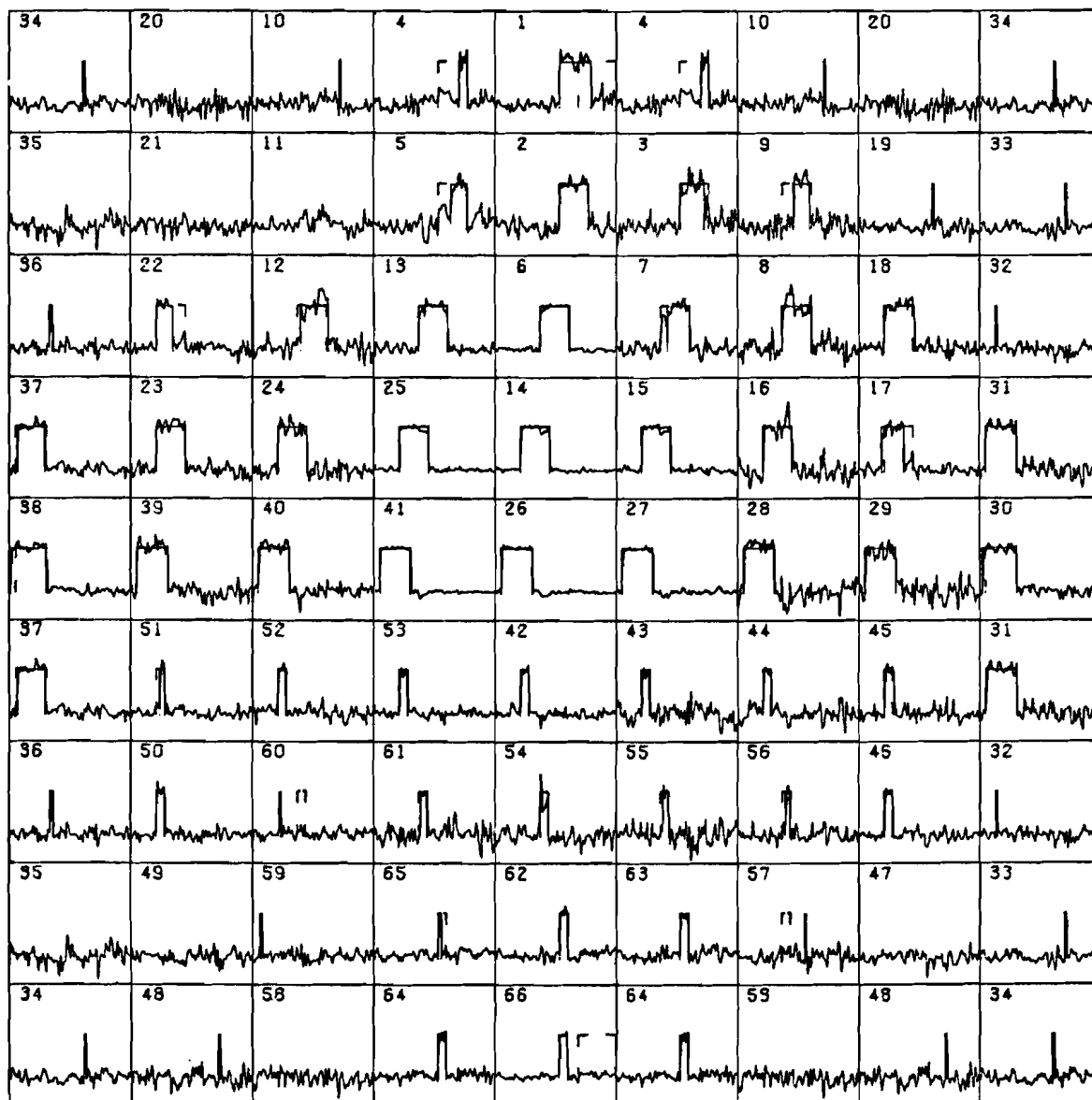


Fig. 12 Estimated double layer on the heart surface  
 ( from simulated skin potentials with noise ),  
 plus the simulated double layer (interrupted line)  
 and the vector  $\underline{b.z}$  (thin line).

In order to check the influence of the number of singular values NSV, that are taken into account, the double layer shall also be estimated, if NSV is equal to respectively 20, 25, 30, 40, and 45. For NSV = 20 and NSV = 45 the estimated double layer, together with the simulated double layer and the vector  $\underline{b.z}$  are plotted in respectively figure 13 and 14. From these figures one can clearly see the influence of the noise in the skin potentials. To get a clear view of the derived results, some characteristics of these results have been presented in table 1.

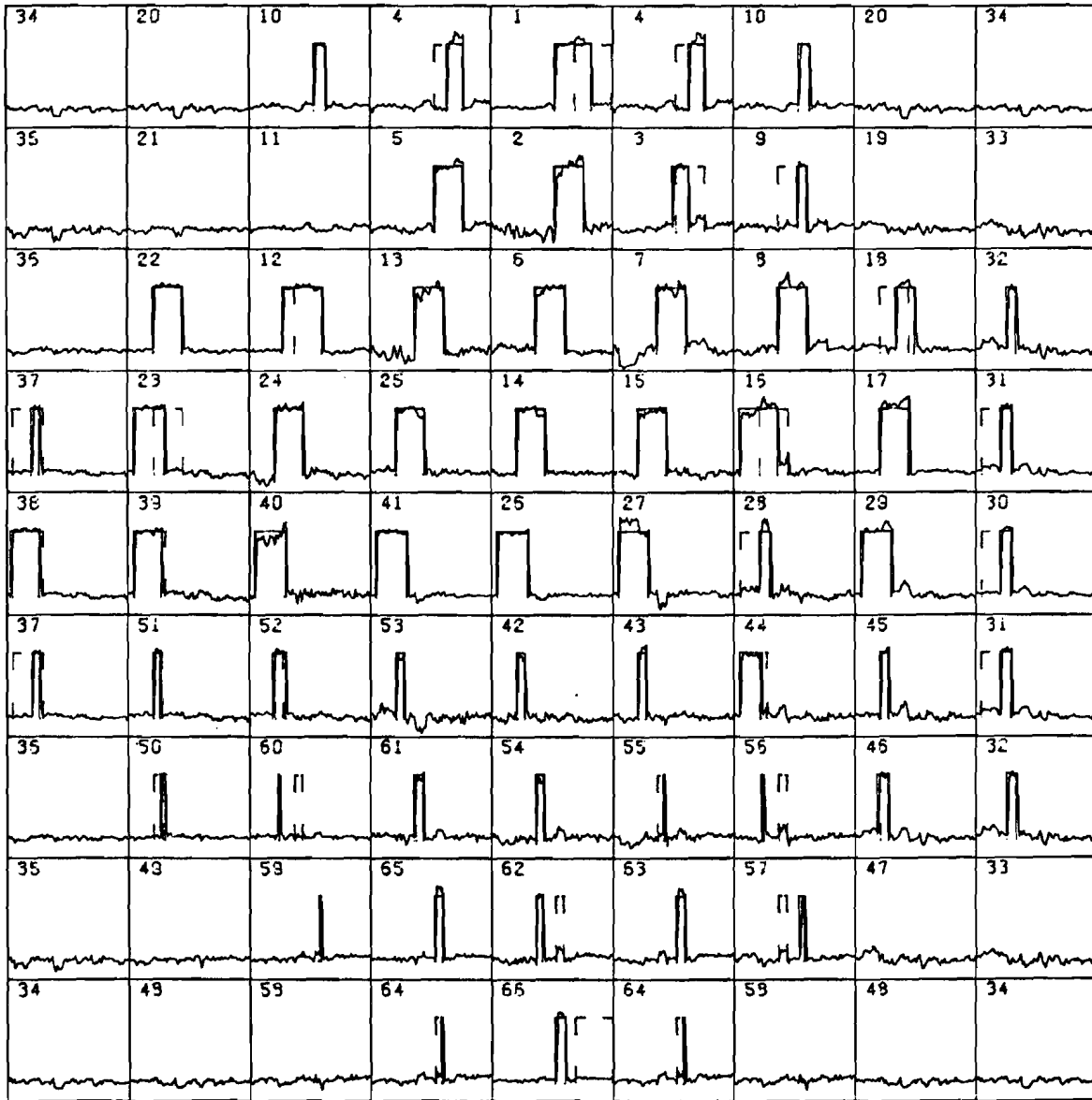


Fig. 13 Estimated double layer on the heart surface  
( from simulated skin potentials with noise ),  
plus the simulated double layer (interrupted line)  
and the vector  $b.z$  (thin line).  
Number of "used" singular values = 20.

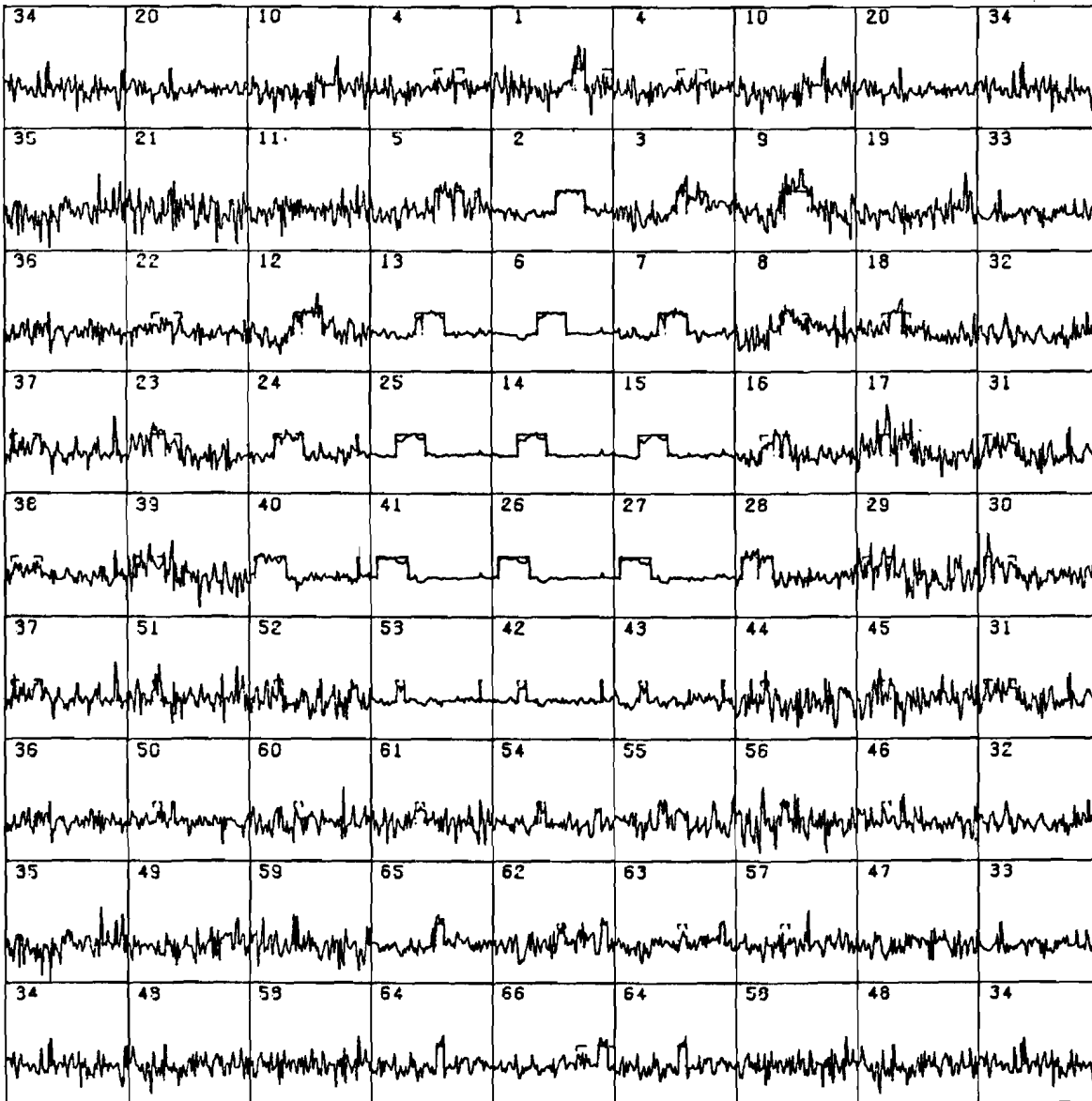


Fig. 14 Estimated double layer on the heart surface (from simulated skin potentials with noise ), plus the simulated double layer (interrupted line) and the vector  $b.z$  (thin line).  
Number of "used" singular values = 45.



NSV	good	wrong start	peaks	bad	b
20	42	5	1	18	12.689
25	40	4	4	18	12.664
30	37	4	6	19	12.943
35	48	3	8	7	12.521
40	30	6	12	18	12.733
45	14	26	14	12	12.896

$$\text{real } b = 4\pi \approx 12.566$$

Table 1 Results of the estimated double layers.

In table 1 are successively indicated:

- the number of points on the heart surface, in which:
  - a) the estimation of the equivalent double layer is good, i.e. whether more than 80% of the double layer activity, which ought to be there, is found, or no activity, which might also not be present, is found;
  - b) the estimation of the equivalent double layer is bad, because of a wrong start situation;
  - c) disturbance peaks occur;
  - d) the estimation of the equivalent double layer is bad, besides the number with a wrong start situation and the number of disturbance peaks;
- the estimated constant b.

From this table can be concluded, that the choice to use only 35 inverse singular values in the estimation of the double layer was a right one. In that case the number of points, in which the double layer is well estimated, is greater than in all other situations. Also the number of points, in which the double layer is estimated badly, is much smaller. Even the number of "wrong start situation" is smallest here. Only the number of points, in which disturbance peaks occur is greater than for example in the case that  $NSV = 20$ . However, an experienced cardiologist should be able to distinguish these calculation errors from a possible heart defect. It is also strikingly, that the estimation of the constant b approximates the real amplitude the nearest if  $NSV = 35$ .

If, finally, the error E in the criterion (29) is put in a diagram as a function of NSV, then can be seen, that this error increases as NSV increases ( see figure 15 ).

This is to impute to:

- a) the increasing influence of the noise ( see for example figure 14 ). Namely, if NSV increases, then more and more relative larger inverse singular values shall be taken into account. This means, that according to (8) the noise in the skin potentials will be multiplied with a greater and greater factor.
- b) a less number of degrees of freedom to estimate the double layer. In this case the estimation algorithm has less space to adjust to the conditions the relative well observable distributions over the heart.

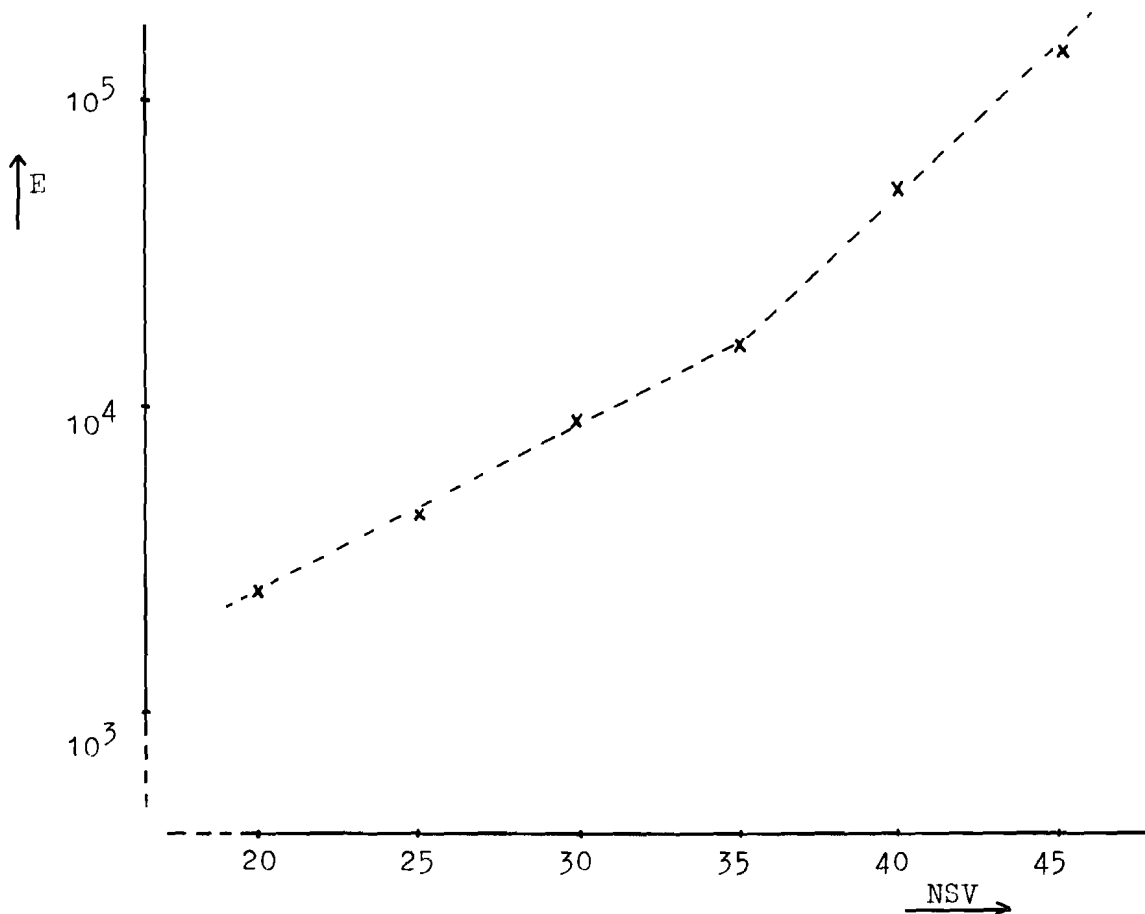


Fig. 15 The error E as a function of NSV (= number of "used" singular values).

Noticeable is the stronger increasing of the error E above NSV = 35. In this part of the diagram the influence of the noise will be dominant, because then distributions are taken into account with a signal to noise ratio less than 1 (see page 16). All in all this error E can not be a criterion to derive a best fit for the estimated double layer, because from table 1 can be found, that the best fit is derived at NSV = 35, while the error E shall decrease if NSV decreases.

---

The estimation of the equivalent double layer is among other things based on the assumption that has been made about the covariance of the fundamental epicardial potential distributions  $V^T \phi_e$  ( see page 15 ). It is allowed to substitute the equivalent double layer, projected on the columns of the matrix  $V$ , instead of the fundamental epicardial potential distributions, because  $V$  is a square orthonormal matrix, so that (12) becomes:

$$E [ \underline{P}_e \cdot \underline{P}_e^T ] = c^2 I \quad (30)$$

where  $\underline{P}_e = V^T \underline{z}_e$ .

In order to check this assumption, the vector  $\underline{P}_e$  will be discretised in the way as described on page 19. The vector  $\underline{P}_e(t)$  will then be written in the matrix  $W$ .

The S.V.D. applied on this matrix will give:

$$W = F G H^T$$

and consequently:

$$E [ \underline{P}_e \cdot \underline{P}_e^T ] = E [ W W^T ] = F G^2 F^T \quad (31)$$

If the above-mentioned assumption should be true, then the diagonal matrix  $G$  should have equal singular values.

However, it appears, that only 8 singular values are nonzero ( see figure 16 ). This means, that only 8 fundamental distributions  $v_i^T \underline{z}_e$  over the heart are of importance in this simulation. So, equation (30) seems not to be true theoretically, but the derived results from the estimation, however, are satisfactorily in practice, so that the real measurements may be processed in a similar way. The more, because in the real situation only about 9 fundamental distributions seem to be dominant, as is shown e.g. in Van der Kam/Damen [21], page 19.

The estimation of the epicardial potentials from measured skin potentials will be discussed in the next chapter.

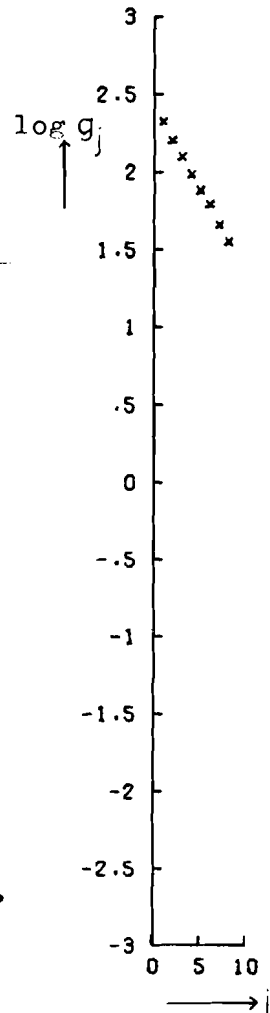


Fig. 16 The singular values of the matrix  $W$ .

5. ESTIMATION OF THE EPICARDIAL POTENTIALS FROM MEASURED SKIN POTENTIALS

The theory, developed in chapter 3, has been checked with the help of a simulated source distribution in chapter 4. Because the results were satisfactorily, it seems to be justified to estimate now the epicardial potentials from real skin potentials. Before passing on to this estimation, it is necessary to make some notes about the measured skin potentials and about the heart-to-skin transfermatrix.

5.1. The Electrocardiogram ( ECG ).

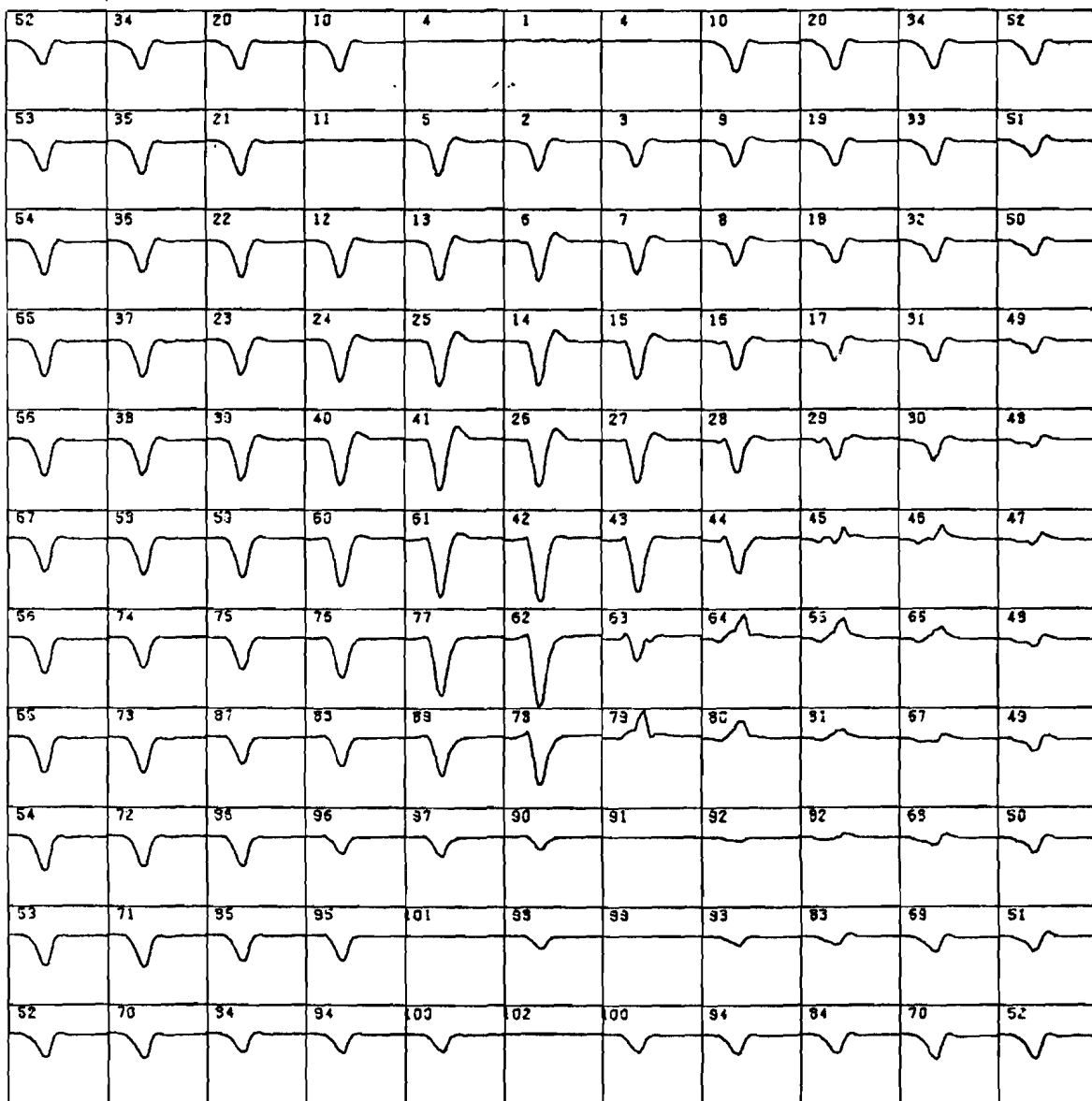


Fig. 17 The measured skin potentials.

In the measuringpoints, as defined in paragraph 2.2., the electrical potentials are measured as a function of the time and supplied to an ECG-amplifier ( see [13] ). The ECG-signal is supposed to be periodic during the measurements, so that on a quasi-stationary basis the signals can be measured in groups. The ECG-signals are simultaneously measured in groups of six on a seven trace analog recorder. After a 10-bit AD-conversion, with a sample time of 1 msec, the signals are read into a computer. Then the signals are corrected for baseline drift by using the silent periods between the complexes. The time alignment is obtained with the help of cross-correlation technics. Finally, per measuringpoint, one complex was averaged out of ten complexes to reduce the influence of the noise.

Figure 17 shows a set of measured skin potentials that have been obtained after the above-mentioned operations. In each square a QRS-complex is plotted as measured at one point on the skin. The total duration is 150 msec.; this is equal to 51 samples with an interval time of 3 msec. Electrodesignal 91 is used as reference signal, while the potentials in the points 1, 4, 11, 82, 99, 101 and 102 could not be measured because of the extremities or are rejected because of a measurement error. The potentials in the remaining 95 points shall be used to estimate the epicardial potentials.

### 5.2. The transfermatrix relating epicardial potentials to skin potentials.

In paragraph 3.2. has been noted, that the relation between epicardial and skin potentials can be realised, under certain assumptions, by a matrix, so that:

$$\phi_s = A \phi_e \quad (4)$$

The calculation of the matrix A shall be briefly explained in this paragraph.

Analogous to what is described in the Appendix for the equivalent double layer can be stated here for the epicardial potentials, so that:

$$\phi_\infty = B \phi_s$$

and: 
$$\phi_\infty = D \phi_e$$

where :  $\phi_\infty$  is a vector, consisting of m elements,  
namely the potentials in m points of an infinitely wide medium;

B is a singular mxm-matrix;

D is a regular mxn-matrix.

The matrices B and D are calculated by Vermeulen [22].  
From these two equations could be derived, that:

$$\phi_s = B^{-1} D \phi_e \quad (31)$$

But the matrix B appeared to be singular, so that it is not possible to invert this matrix. However, it is possible to apply the S.V.D. on the matrix B, so that:

$$B = K L M^T$$

where : K and M are leftunitary mxm-matrices;

L is a mxm-diagonal matrix, of which the last element is equal to zero; so:

$$L = \text{diag}(l_1, l_2, \dots, l_{m-1}, 0)$$

The pseudo-inverse of B can be defined, according to (2), as follows:

$$B^{-1} = M L_r^{-1} K^T \quad (32)$$

where  $L_r^{-1}$  is the inversion of the diagonal matrix L with the restriction that the last element is defined equal to zero; so:

$$L_r^{-1} = \text{diag}(l_1^{-1}, l_2^{-1}, \dots, l_{m-1}^{-1}, 0)$$

So, assimilating of equation (4) and (31) and making use of equation (32) gives:

$$A = M L_r^{-1} K^T D \quad (33)$$

In the last paragraph it appeared, that the potentials in 7 points on the torso could not be measured. Consequently, these unmeasurable elements of the vector  $\phi_s$  should be "deleted", so that this vector has only 95 elements.

The transfermatrix A, however, is calculated for 102 elements of the vector  $\phi_s$ , so that from A the rows, corresponding to the deleted elements of the vector  $\phi_s$ , should also be eliminated. In this case, equation (4) will become:

$$\phi_{s, \text{red}} = A_{\text{red}} \phi_e$$

where the subscript red stands for reduced.

It is obvious, that the S.V.D. shall be applied to this reduced transfermatrix as described in paragraph 3.2. The singular values of this transfermatrix are represented in figure 18.

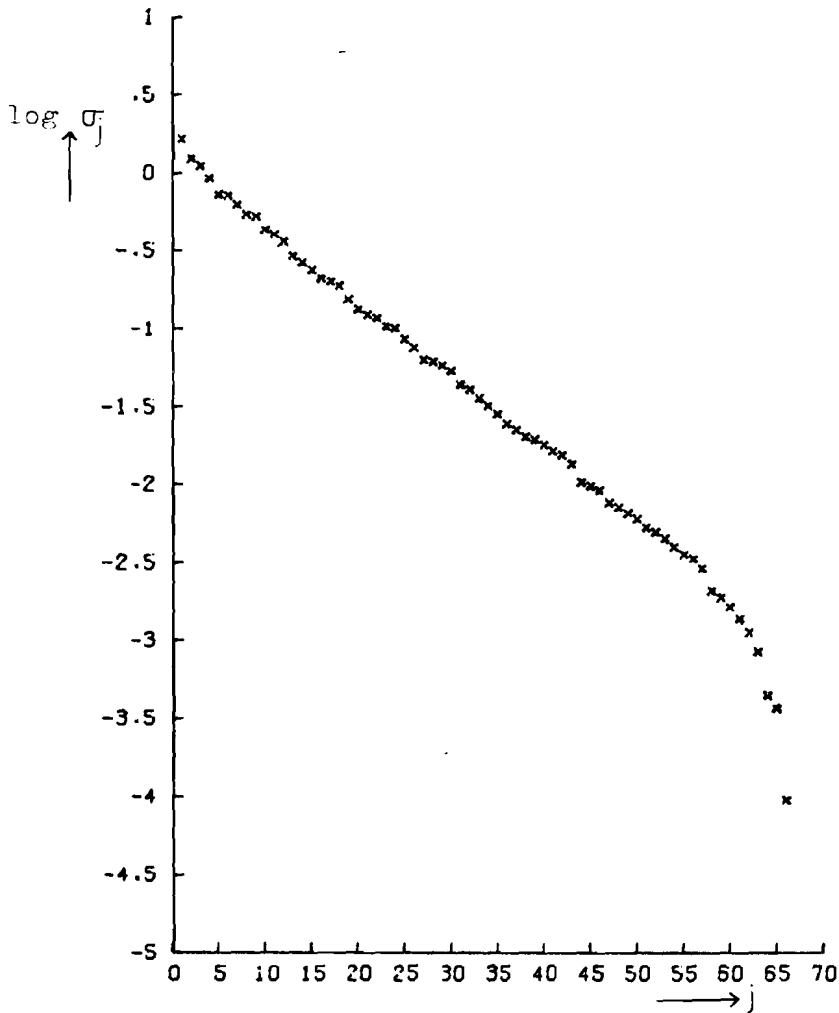


Fig. 18 The singular values of the reduced transfer matrix.

### 5.3. Results.

The estimation of the epicardial potentials from the skin potentials progresses completely analogous to the estimation of the equivalent double layer, as described in paragraph 4.3. So, firstly the number of inverse singular values, that should not be set equal to zero, will be calculated from the noise influence. This number appears to be equal to 34, so that 32 inverse singular values are set to zero.

The finally estimated epicardial potentials, together with the vector  $b.z$ , are plotted in figure 19.

From this can be concluded, that the estimation of the epicardial potentials is not yet successful. For example, the propagation of the depolarisation-wave on the epicardium is not perceptible. The estimated propagation can better be seen in figure 20, wherein at some special moments the points are indicated, which are active at that moment.

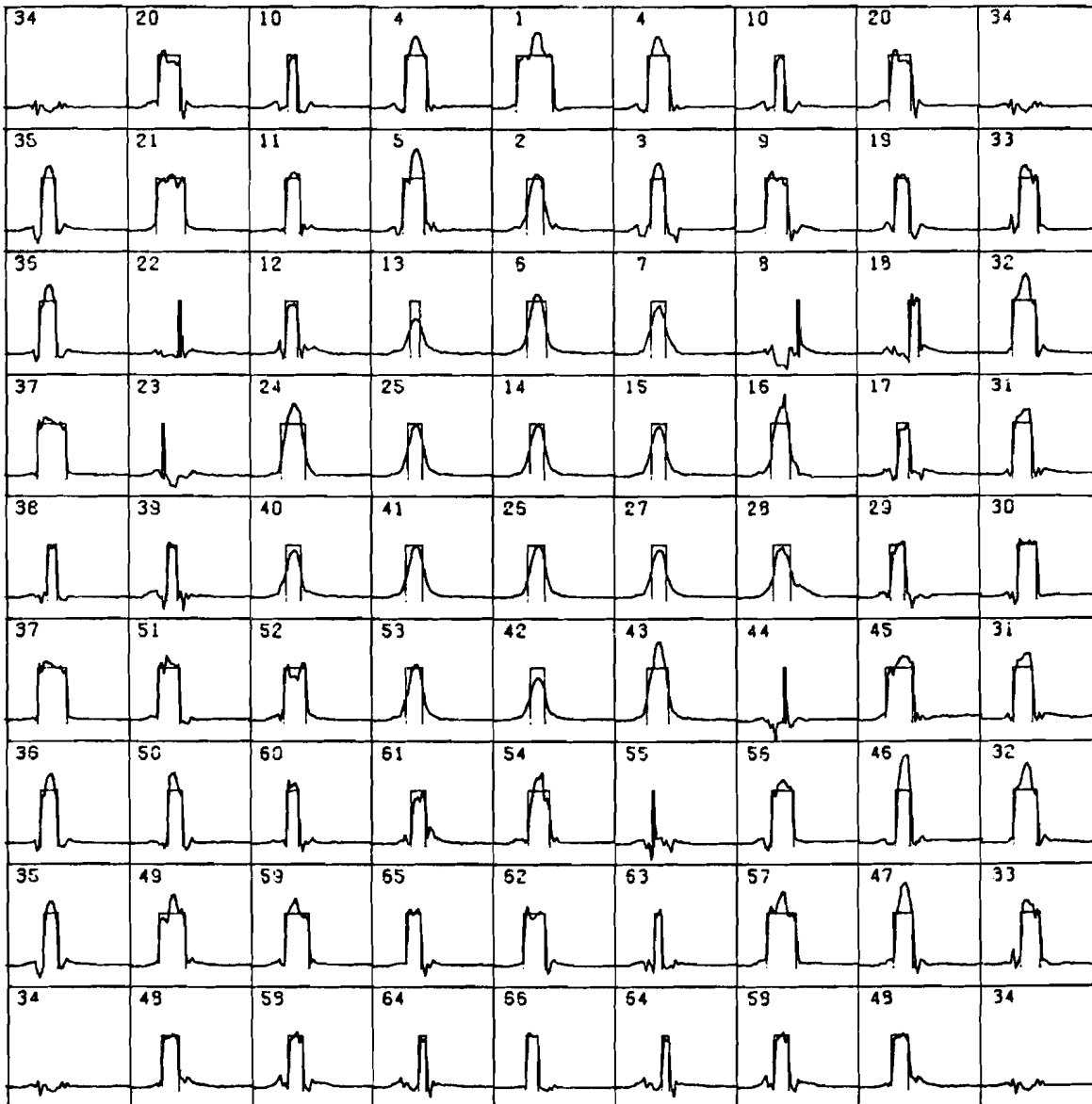


Fig. 19 Estimated epicardial potentials and the vector  $b.z$  (thin line).

These bad results are probably due to the facts:

- a) A bad determination of the geometry and position of the heart in the body. These data have a great influence at the calculation of the transfer matrix.
- b) The influence of the inhomogeneities is taken no account of. In which way these inhomogeneities could affect the epicardial potentials is not very clear, but that they shall have any influence is obvious.
- c) The on-off character of the sources is a restriction too sharp in reality.
- d) The estimation of 34 relevant singular values may be too low, because the noise in the skin potentials now has hardly any influence, as can be concluded from figure 19.

If in future one would determine the epicardial potentials better, it is necessary to take these considerations into account.



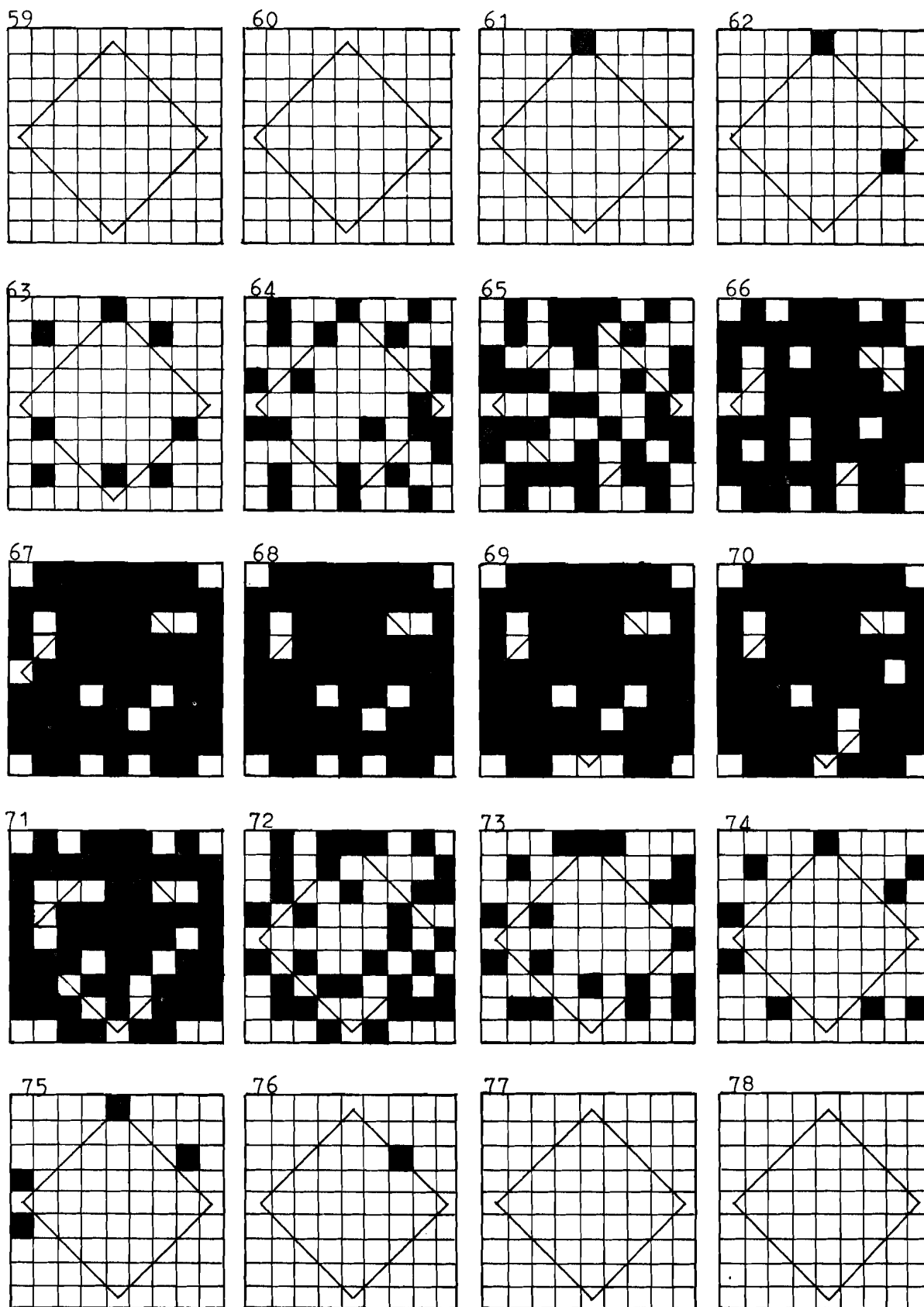


Fig. 20 Estimated propagation of the depolarisation-wave in the time interval 59 - 78. Each square is the projection of the heart surface.

## CONCLUSIONS

The S.V.D. applied to the heart-to-skin-transfer matrix yields fundamental potential distributions on the heart surface and on the skin. These distributions are related to each other via transfer coefficients, called the singular values. These singular values are a measure for the observability of the fundamental potential distributions on the epicard. A rough estimate yields, that only 34 of the 66 distributions on the epicard cause skin potentials, which lie above the noise level. Consequently only 34 distributions can be estimated reliably. The remaining 32 distributions have to be ignored, so that 32 degrees of freedom are obtained. These degrees of freedom can be used to estimate the epicardial potentials better with the help of the a priori information about the electrical heart activity.

The choice of the number of non-observable epicardial patterns has been based among other things on the assumption, that all (66) fundamental distributions on the heart have an equal chance of occurrence. In the simulation it appeared, that only 8 distributions over the heart are of importance. However, the assumption of 66 equi-important patterns turns out to lead to the best estimation of an equivalent source distribution from simulated skin potentials. This needs not to be the case in the real situation.

The estimation of the epicardial potentials from measured skin potentials gives bad results, though the influence of the noise was sufficiently reduced. For example, the potentials in some points on the epicard have no correlation in time with their neighbouring points, in other words, no perceptible propagation of the depolarisation-wave. These bad results can be imputed to the following facts:

- Bad determination of the geometry and position of the heart in the body. At the calculation of the heart-to-skin-transfer matrix, this will have a great influence.
- The electrical properties of the inhomogeneities was not implemented in the estimation algorithm. Though the influence of these inhomogeneities is not very clear, it is obvious, that this is not a negligible factor.
- Probably the on-off character of the sources is a restriction too sharp for reality.
- The estimation of 34 relevant singular values of the transfer matrix may be too low.

Of course the implementation of these considerations in the estimation algorithm shall be a problem apart, but it shall also be necessary to derive more realistic results in practice. Nevertheless, under these conditions, the possibility of identification has been shown in the model to model adjustments.

It would also be interesting to investigate the influence of the density of points on the epicardium and on the torso. Namely, it was estimated, that only 34 of the 66 distributions over the heart could be estimated reliably. Probably this number shall increase, if the density of the points on the heart surface shall become greater. If also the density of the point distribution on the torso and then especially on the precordial side shall increase, then this should mean, that higher space frequencies could be measured.

On the contrary, it is not very likely, that these high space frequencies are present on a relevant level in the epicardial potentials. So, this also contradicts the assumption, that all distributions over the heart surface have an equal chance of occurrence. In practice, namely, only 9 independent patterns on the heart surface are found [21].

LITERATURE

- [1] Scher, A.M., Young, A.C. and Meredith, W.M.,  
"Factor Analysis of the Electrocardiogram",  
Circ. Res. Vol.8, May 1960, pp. 519...526.
- [2] Young, T.Y. and Huggins, W.H.,  
"The Intrinsic Component Theory of Electrocardiography",  
IRE Trans. Bio-Med. Eng., Vol.BME-9, Oct. 1962, pp. 214...221.
- [3] Horan, L.G., Flowers, N.C. and Brody, D.A.,  
"Principal Factor Waveforms of the Thoracic QRS-complex",  
Circ. Res. Vol.15, Aug. 1964, pp. 131...145.
- [4] Plonsey, R.,  
"Bioelectric Phenomena",  
Mc Graw-Hill, New York, 1969.
- [5] Barr, R.C., Pilkington, T.C., Boineau, J.P. and Rogers, C.L.,  
"An inverse Electrocardiographic Solution with an ON-OFF Model",  
IEEE Trans. Bio-Med. Eng., Vol.BME-17, No.1, Jan. 1970,  
pp. 49...56.
- [6] Francis, D.B.,  
"Multipole Models of the Human Heart",  
Dissertation Carnegie-Mellon Univ., 1970,  
Univ. Microfilms Inc., Ann Arbor, Michigan, U.S.A.
- [7] Golub, G.H. and Reinsch, C.,  
"Singular Value Decomposition and Least Squares Solutions",  
Num. Math. Vol.14, 1970, pp. 403...420.
- [8] Barr, R., Spach, M. and Giddens, H.,  
"Selection of the Number and Positions of Measuring Locations  
for Electrocardiography",  
IEEE Trans. Bio-Med. Eng., Vol.BME-18, No.2, March 1971,  
pp. 125...138.
- [9] Martin, R.O. and Pilkington, T.C.,  
"Unconstrained Inverse Electrocardiography: Epicardial  
Potentials",  
IEEE Trans. Bio-Med. Eng., Vol.BME-19, No.4, July 1972,  
pp. 276...285.
- [10] Damen, A.A.H.,  
"A Comparative Analysis of Several Models of the Ventricular  
Depolarisation; Introduction of a String Model",  
Report of University of Technology, No.73-E-41,  
Eindhoven, The Netherlands, 1973.
- [11] Damen, A.A.H.,  
"Some Notes on the Inverse Problem in Electrocardiography",  
Report of University of Technology, No.74-E-48,  
Eindhoven, The Netherlands, 1974.
- [12] "Measurements in Medical Science 1", (in Dutch),  
Lecture Syllabus, University of Technology,  
Eindhoven, The Netherlands, 1975.

- [13] Burema, T.,  
"An 8-Channel ECG-Amplifier;  
Automatisation and Testing of an ECG-Assimilation System",  
(in Dutch ),  
Intern Report of University of Technology, Group Measurement and  
Control, Department of Electrical Engineering,  
Eindhoven, The Netherlands, Nov. 1975.
- [14] Damen, A.A.H.  
"Epicardial Potentials Derived from Skin Potential Measurements",  
Report of University of Technology, No.76-E-64,  
Eindhoven, The Netherlands, 1976.
- [15] Van Schaik, J.W.M.  
"The Reproducibility of the Cardiogram", (in Dutch).  
M.Sc. thesis, University of Technology,  
Eindhoven, The Netherlands, Nov. 1976.
- [16] Nelson, C.V. and Geselowitz, G.B.,  
"Theoretical Basis of Electrocardiology",  
Clarendon Press, Oxford, 1976.
- [17] Barr, R., Ramsey, M. and Spach, M.  
"Relating Epicardial to Body Surface Potential Distributions by  
means of Transfer Coefficients based on Geometry Measurements",  
IEEE Trans. Bio-Med. Eng., Vol.BME-24, No.1, Jan. 1977, pp.1...11.
- [18] Stroeken J.  
"Estimation of the depolarisation pattern from ECG-signals",  
(in Dutch ),  
M.Sc. thesis, University of Technology,  
Eindhoven, The Netherlands, 1978.
- [19] Veltkamp, G.W.,  
"Matrix Theory", (in Dutch)  
Lecture Syllabus, University of Technology,  
Department of Mathematical Engineering,  
Eindhoven, The Netherlands, 1977.
- [20] Nicola, V.F.,  
"Planar Projection for Closed Surfaces in 3-dimensional Space",  
Report of training work, University of Technology,  
Eindhoven, The Netherlands, 1977.
- [21] Van der Kam, J.J. and Damen, A.A.H.,  
"Observability of electrical heart activity studied with the  
singular value decomposition",  
Report of University of Technology, No.78-E-81,  
Eindhoven, The Netherlands, Febr. 1978.
- [22] Vermeulen, J.W.M.,  
"On the Determination of Electrical Epicardial Potentials from  
Skin Potentials and Geometry Data",  
M.Sc. thesis, University of Technology,  
Eindhoven, The Netherlands, Febr. 1978.
-

ACKNOWLEDGEMENT

The author is much indebted to Prof. dr. ir. P. Eykhoff and to Ir. A. Damen for their enormous support and guidance during this study.

APPENDIX: Notes about the calculation of the transfermatrix relating double layers to skin potentials.

With the help of Green 's Second identity it is possible to derive continuous relations between the unbounded medium potentials <sup>\*\*</sup> and the skin potentials. The same holds for the relation between the unbounded medium potentials and the equivalent double layer. These relations can be discretised and lead to:

$$\phi_{\infty} = B \phi_s \quad (A1)$$

$$\phi_{\infty} = C \underline{z}_e \quad (A2)$$

where :  $\phi_{\infty}$  is a vector, consisting of m elements, namely, the potentials in m points of an infinitely wide medium;

$\phi_s$  is a vector, consisting of m elements, namely, the potentials in m points on the skin;

$\underline{z}_e$  is a vector, consisting of n elements, namely, the double layer activity in n points on the heart surface and  $n \leq m$ ;

B and C are respectively mxm- and mxn-matrices, calculated by Vermeulen [22].

The matrices B and C both have a zero singular value and an unit vector as eigenvector, because the rowsums <sup>\*\*\*</sup> of the matrices B and C are zero ( see [22] ). Physically this means, that the skin potentials can be defined except for a constant level and a constant double layer will not cause any potential field out side the double layer surface.

The S.V.D. of both matrices will give:

$$B = K L M^T \quad (A3)$$

$$C = F G H^T \quad (A4)$$

where : F, H, K and M are respectively leftunitary mxn-, nxn-, mxm- and mxm-matrices;

G and L are respectively nxn- and mxm-diagonal matrices, of which the last singular value is equal to zero;

so:

$$G = \text{diag}( g_1, g_2, \dots, g_{n-1}, 0 )$$

$$L = \text{diag}( l_1, l_2, \dots, l_{m-1}, 0 )$$

-----  
<sup>\*\*</sup> An unbounded medium potential in a point is equal to the potential, which would be in that point if the medium was infinitely wide.

<sup>\*\*\*</sup> rowsum = sum of all elements of a row.

The last column of the matrix  $M (= [M]_m)$  and the last column of the matrix  $H (= [H]_n)$  are equal to an unit vector  $\underline{e}$ , ( $\underline{e}^T = (1, 1, \dots, 1)$ ). The physical significance of the last column of the matrix  $K (= [K]_m)$  and the last column of the matrix  $F (= [F]_n)$  is not so easy to show. But as will turn out at the end of this appendix, this is of no importance.

Inversion of (A1) will, according to (A3) and (2) give:

$$\underline{\phi}_s = M L_r^{-1} K^T \underline{\phi}_\infty \quad (A5)$$

where  $L_r^{-1}$  is the inverse of matrix  $L$ , with the restriction, that the inverse of the last element of  $L$  is defined equal to zero; so:

$$L_r^{-1} = \text{diag}(l_1^{-1}, l_2^{-1}, \dots, l_{m-1}^{-1}, 0)$$

This means, that the columns  $K_m$  and  $M_m$  are neglected in the inversion, so that for the calculated skin potentials it never can hold, that  $\underline{\phi}_s = \underline{e}$ .

Substitution of (A2) in (A5) and using (A4) gives:

$$\underline{\phi}_s = M L_r^{-1} K^T F G H^T \underline{z}_e \quad (A6)$$

The total matrix  $M L_r^{-1} K^T F G H^T$  can be decomposed with the help of the S.V.D., so that (A6) becomes:

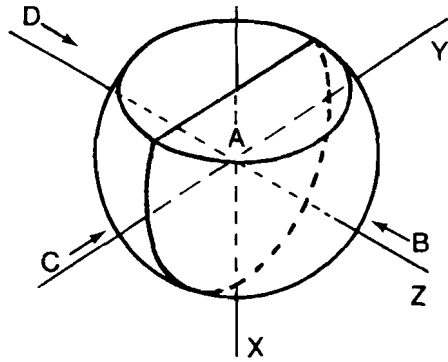
$$\underline{\phi}_s = U Q V^T \underline{z}_e \quad (A7)$$

It may be clear, that the last element of the nxn-diagonal matrix  $Q$  is equal to zero. Likewise the last column of the matrix  $V = [V]_n = [H]_n = \underline{e}$ .

The other way around it holds, that the zero space of the adjoint transformation  $H G F^T K L_r^{-1} M^T$  is equal to  $[M]_m = \underline{e}$ . Because the matrix  $U$  is not square, it is not necessary, that the last column of the matrix  $U (= [U]_n)$  is equal to the unit vector. However it turns out, that the unit vector stands perpendicular on the columns of the matrix  $U$ , including the last one, so that  $\underline{e}^T \underline{\phi}_s = 0$ .

From this it can be concluded, that the calculated skin potentials, from a double layer on the heart surface, are on the average equal to zero. If the skin potentials should include a constant, then this constant will be filtered out by  $[U]_n^T$ . Anyhow the influence of the product  $[F]_n^T \cdot [K]_m$  is of no importance.





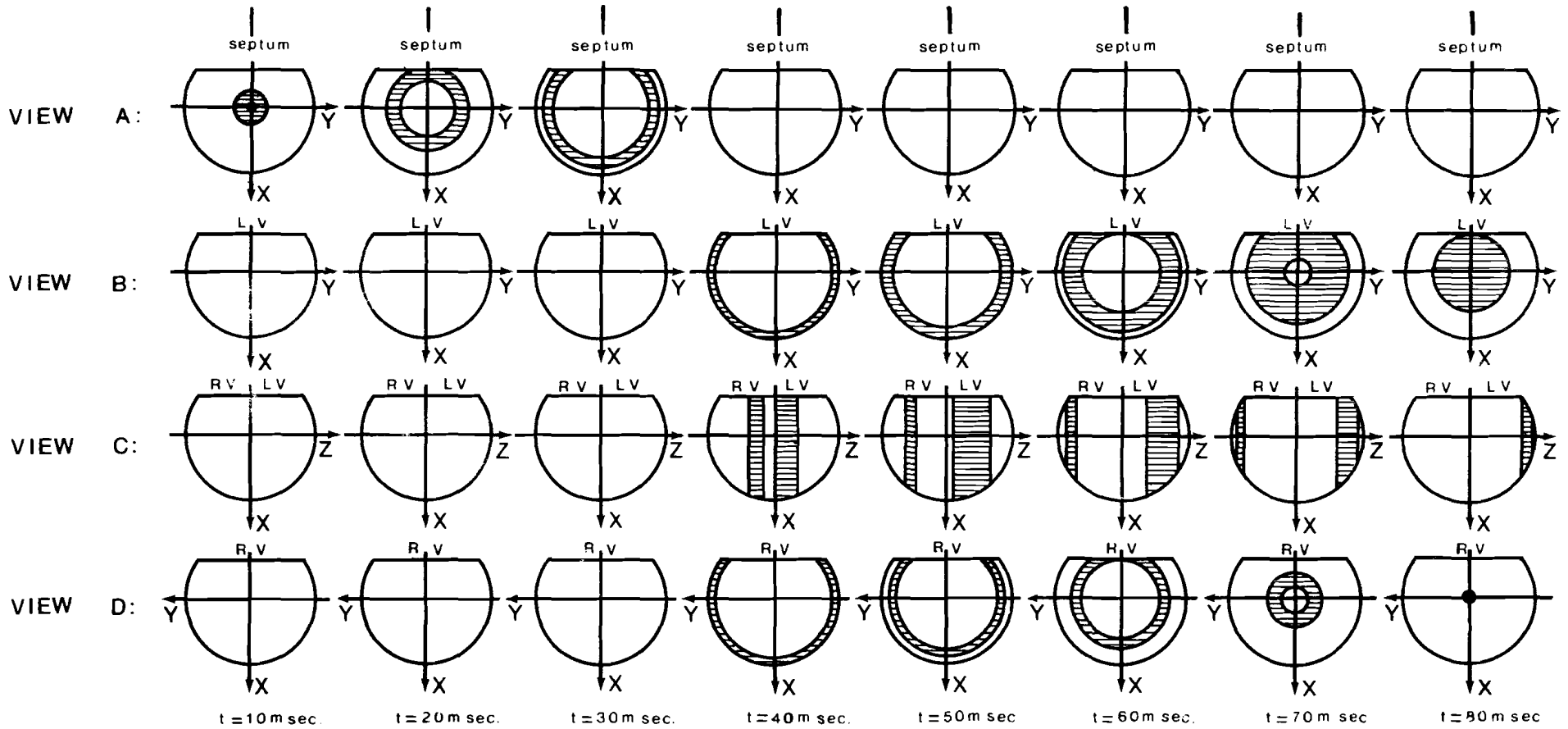
The double layer (shaded areas) at several moments.

View A: The septum seen from the positive z-axis. (left ventricle is omitted)

View B: The left ventricle seen from the positive z-axis.

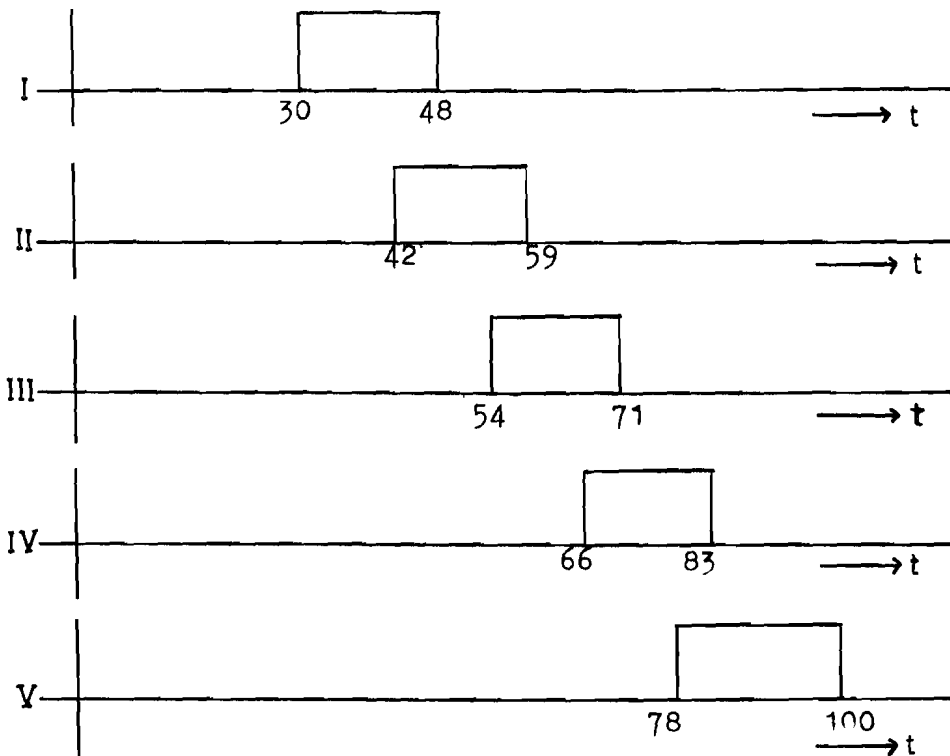
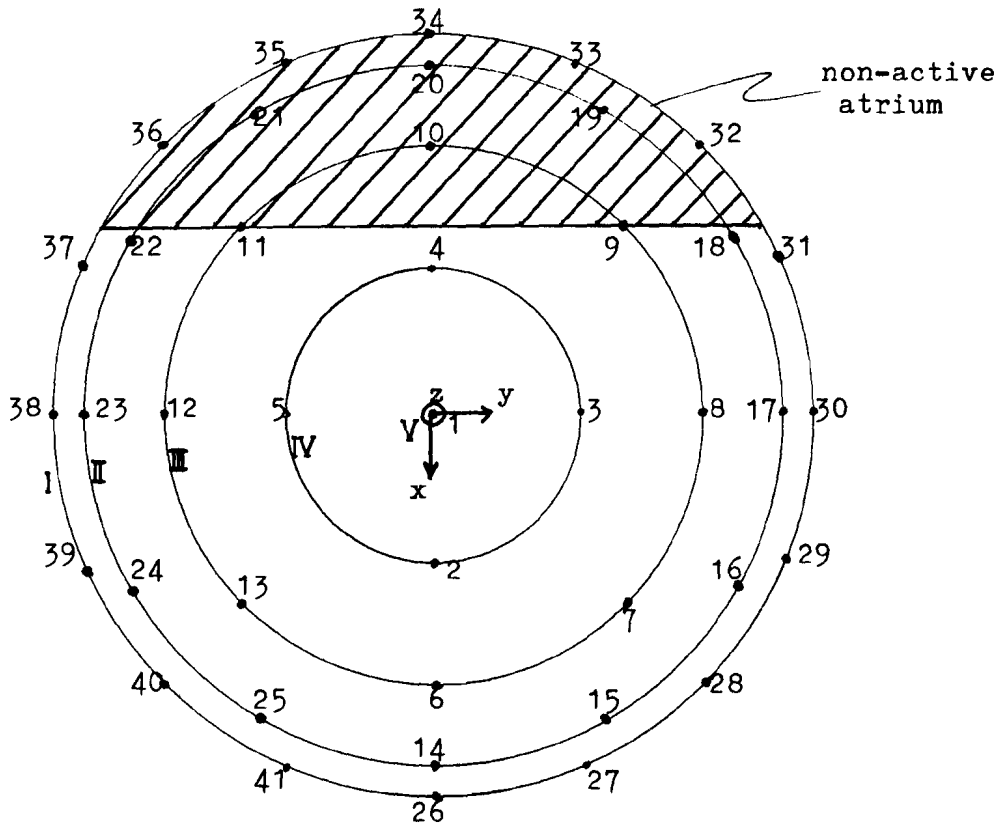
View C: Anterior view from the negative y-axis.

View D: The right ventricle seen from the negative z-axis.



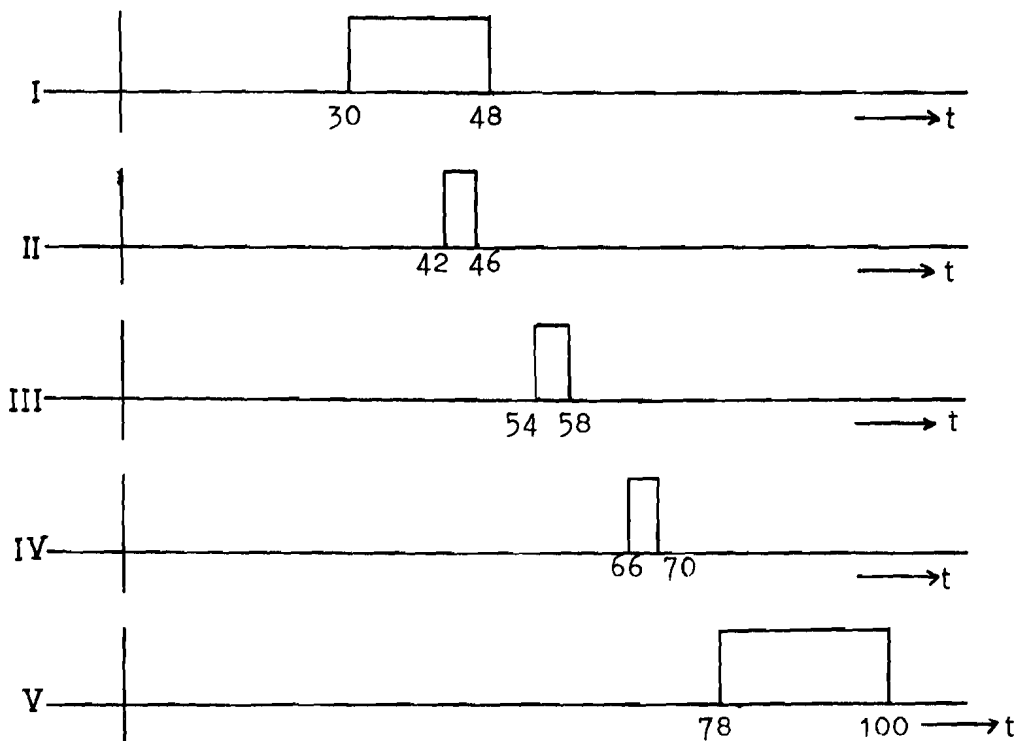
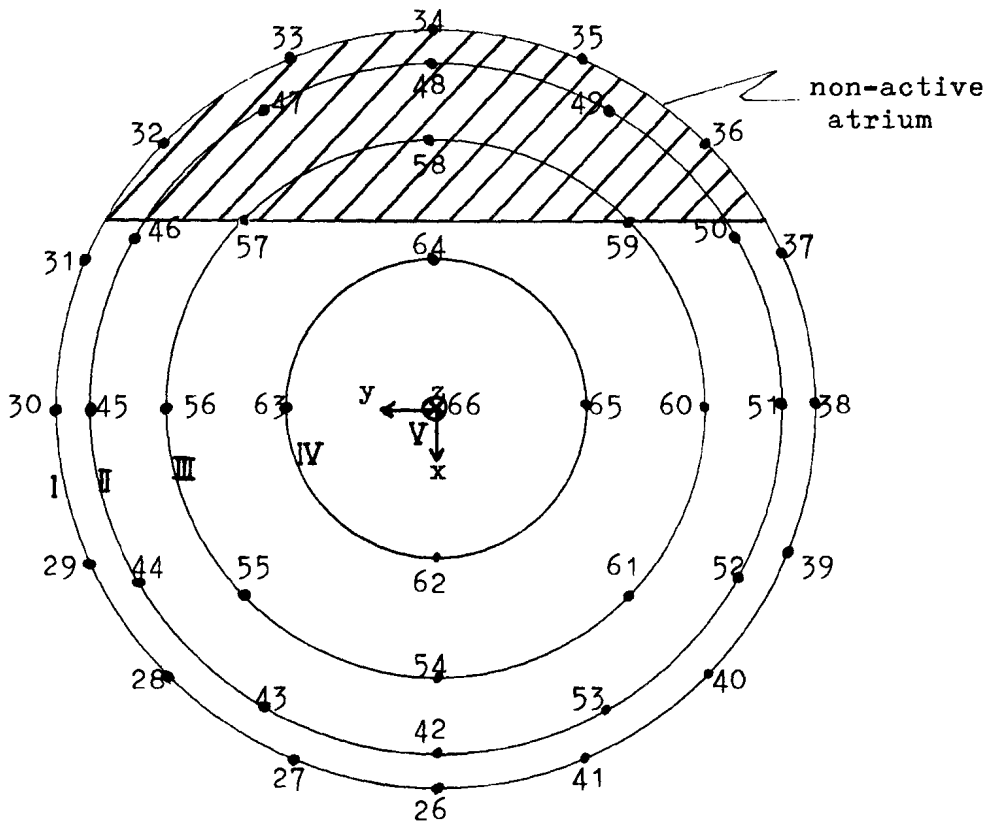
ANNEX 1. The course of the equivalent double layer on the heart surface.

ANNEX 2. The course of the equivalent double layer in the points on the left ventricle.



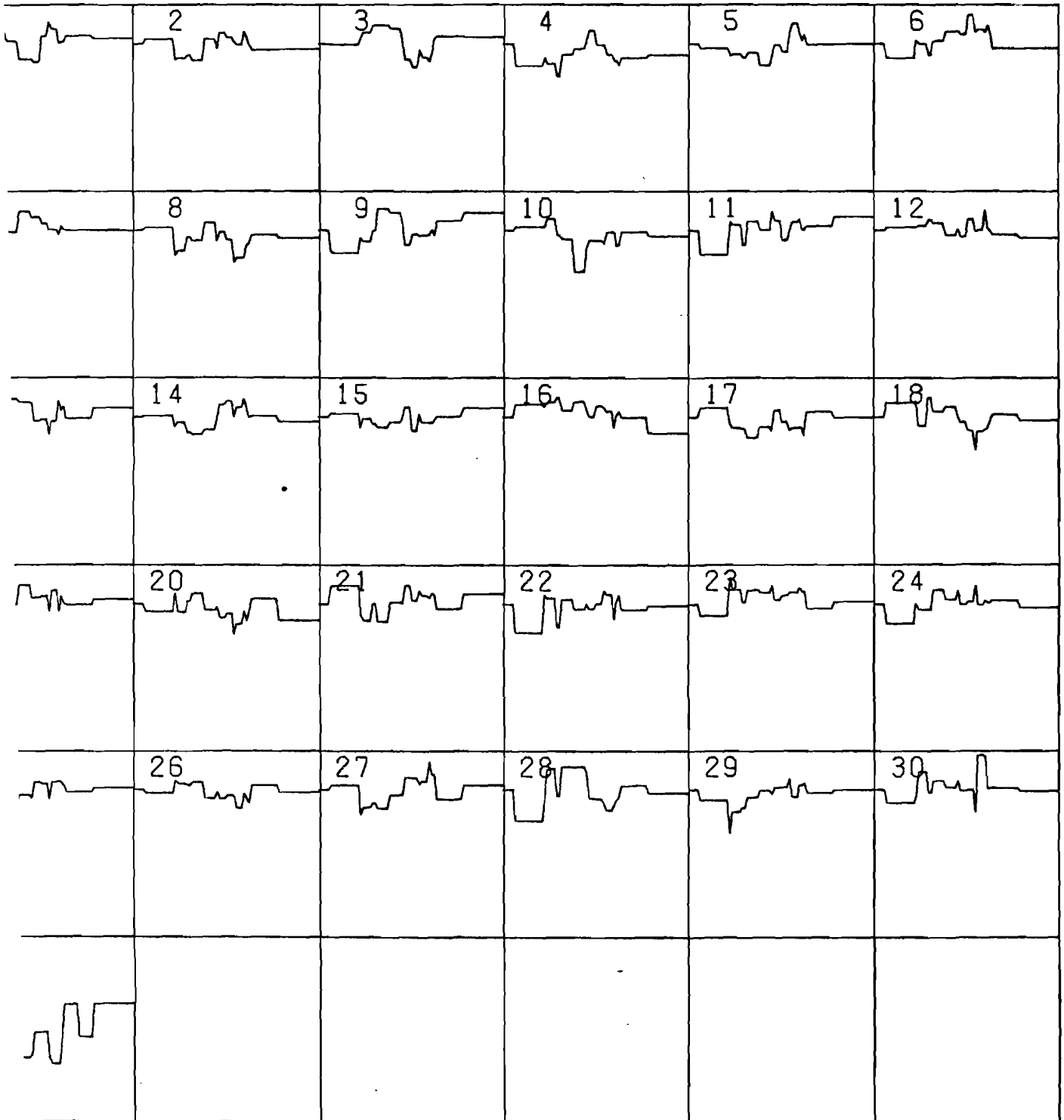
(N.B. The circles connect the points, which are active at the same time).

ANNEX 3. The course of the equivalent double layer in the points on the right ventricle.



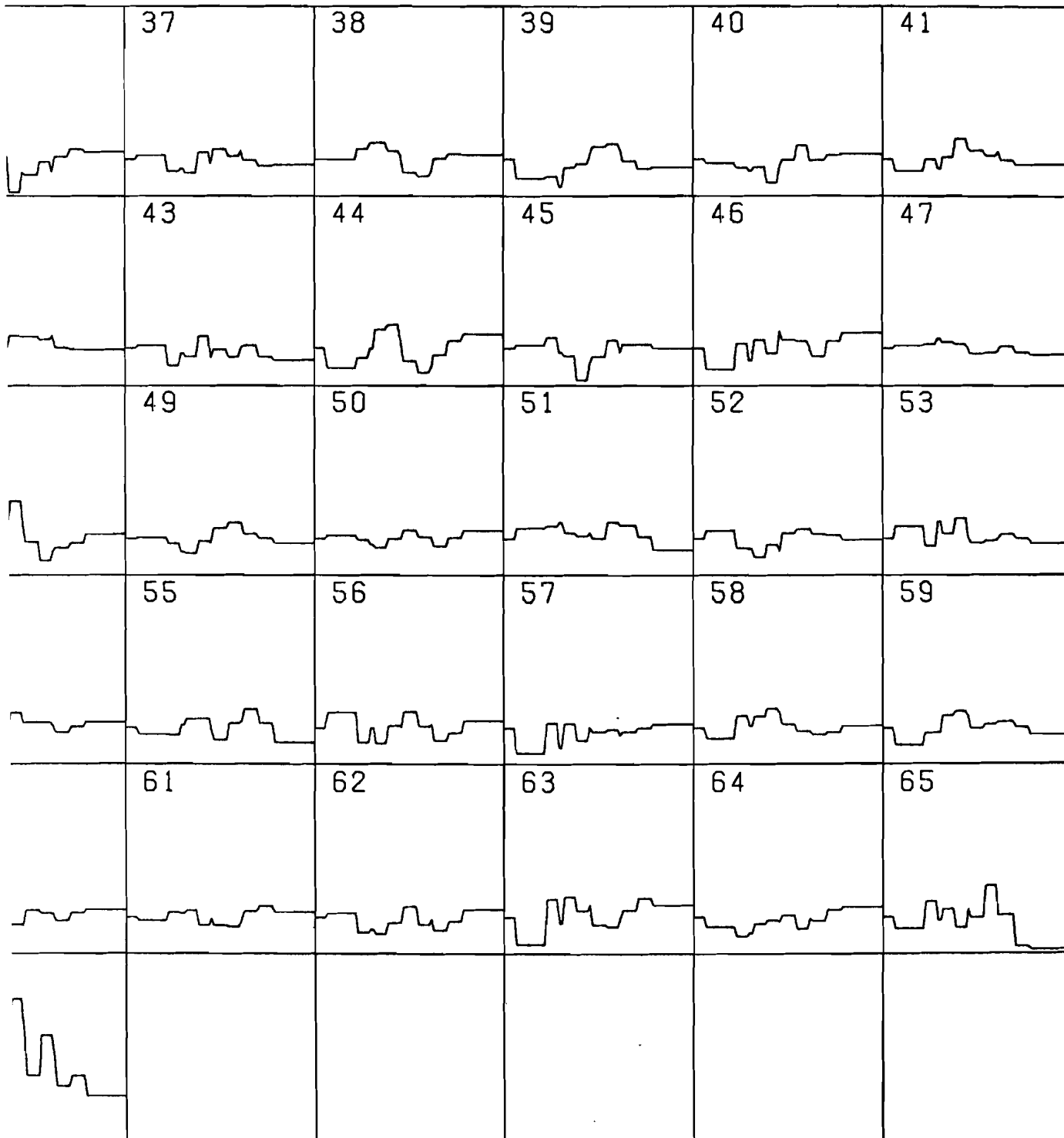
(N.B. The circles connect the points, which are active at the same time).

ANNEX 4. Part of the estimated source distribution on the heart in the simulated noise-free case.



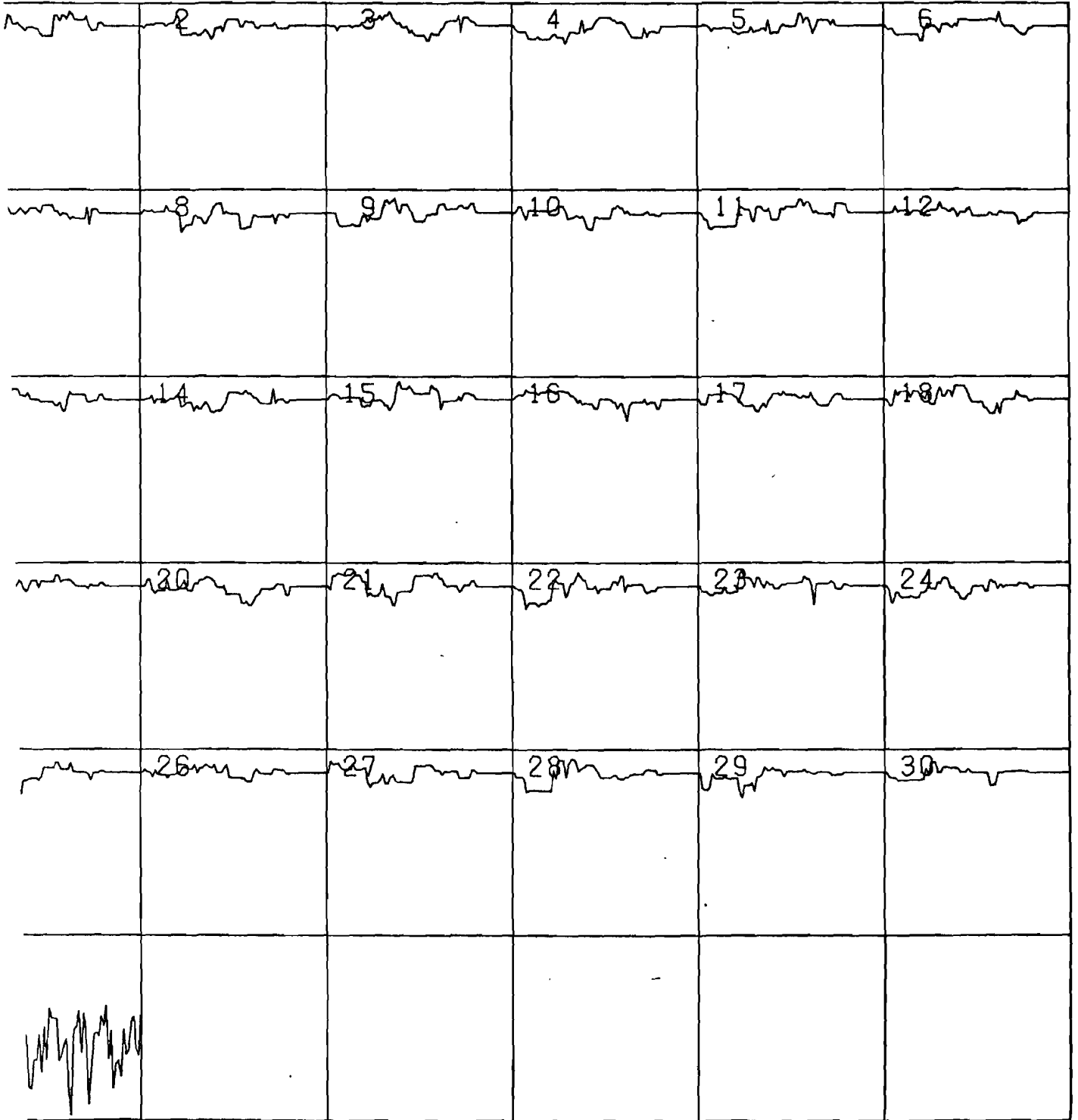
Each square contains an estimated fundamental double layer distribution over the heart as a function of time. The vertical scale is the same in all squares.

ANNEX 5. Part of the simulated source distribution on the heart.



Each square contains a simulated fundamental double layer distribution over the heart as a function of time. The vertical scale is the same in all squares.

ANNEX 6. Part of the estimated source distribution on the heart in the simulated noisy case.



Each square contains an estimated fundamental double layer distribution over the heart as a function of time. The vertical scale is the same in all squares.